New Journal and we have not received input yet 32 (2022) 101242

Contents lists available at ScienceDirect

Thermal Science and Engineering Progress

journal homepage: www.elsevier.com/locate/tsep

# Mixed convection phenomenon in packed beds: A comprehensive review

Gazy F. Al-Sumaily [a,c,*], Hayder A. Dhahad [b], Mark C. Thompson [c]

[a] Energy and Renewable Energies Technology Centre, University of Technology, Iraq
[b] Mechanical Engineering Department, University of Technology, Iraq
[c] Department of Mechanical and Aerospace Engineering, Monash University, Australia

ARTICLE INFO

*Keywords:*
Mixed convection
Porous media
Channels
Darcy model
Non-Darcy model
LTE and LTNE models

ABSTRACT

This review summarises first the studies that have been performed to date for establishing a suitable model for mixed convection phenomenon in packed beds with working fluids include some simplifying assumptions such as local thermal equilibrium ($LTE$) condition, neglect of channelling effect, and neglect of thermal dispersion effect. It was found that most of these studies are based on Darcy's model for the flow and on an averaged single equation model ($LTE$) for the energy equation with using the Boussinesq approximation to represent the variation in fluid density. Theoretical, numerical, or experimental studies, or studies which combine these approaches, are reviewed and for various 2- or 3-dimensional geometries such as horizontal, vertical or inclined parallel plate channels, ducts, cylinders, annuli, etc. In addition, the literature showed that there has been resealable efforts exerted to report works on the non-Darcian mixed convection, in which the effects of boundary, inertia, porosity variation, and inclusion of thermal dispersion under local thermal equilibrium condition ($LTE$) or under thermal non-equilibrium condition ($LTNE$).

## 1. Introduction

The transport process through a porous media has been the topic of numerous studies over many decays. The intensive interest in this problem comes from the sophisticated phenomenon associated with the energy transport during the solid matrix of porous media. Indeed, the existence of such intricate solid structure in the track of the fluid flow expands the liaison surface area, and hence augments the capability of the thermal system to transfer energy [1]. Natural and manufactured porous materials have a broad range of engineering applications in contemporaneous technology. Such implementations can be found in areas such as heat exchangers, solar collectors, geothermal engineering, coal combustors, chemical catalytic reactors, building thermal insulations, petroleum reservoirs, injection moulding, industrial and agricultural water distribution, drying technology, die filling, electronic cooling, heat pipe technologies, energy storage units, food processing, and several other applications, see for example [2–5]. Despite the fact that the flow mechanism inside porous media has preoccupied engineers, geophysicists, and scientists since the beginning of the last century, the phenomenon of convection energy transport has achieved the situation of a separate field of research only within the past few decades.

In fact, the fluid dynamics during porous media is a comparatively old subject. Four principal stages can be recognised from an overview of the sequential evolution of fluid flow within a saturated porous medium theory. The first model was introduced by Darcy [6] who developed a linear relationship well-recognised as Darcy's law, which describes the fluid motion in boundless porous media. Indeed, the Darcy's law demonstrates only the influence of linear frictional drag as a consequence of existence the solid matrix of porous media, and ignores the effects of inertial forces and solid boundaries. After that, the capability range of Darcy's law was developed in the second major stage by Forchheimer [7]. He added a high-order velocity term that represents the inertial effects of porous media to model the nonlinear connection between the pressure gradient and the flowing fluid. Thereby, the Darcy–Forchheimer model has become significant for modelling the flow velocity in porous media with high-porosity or for fluids with lower viscosity. Moreover, the existence of an external solid boundary results in a concept of the momentum boundary layer within the flow field. In spite of the fact that the effect of solid boundary is restricted in a slim momentum boundary layer and acts a trivial function in the general flow consideration, its influence on energy transport might be rather crucial. This effect is further distinguished when the thermal boundary layer having a thickness of the same order or less than that of the momentum boundary layer. This is supposed to happen in heavy fluids with high Prandtl numbers and large pressure differences such as engine oils. Therefore, this effect was added to the Darcy model as

* Corresponding author at: Energy and Renewable Energies Technology Centre, University of Technology, Iraq.
*E-mail addresses:* gazy.alsumaily@monash.edu (G.F. Al-Sumaily), 10592@uotechnology.edu.iq (H.A. Dhahad), mark.thompson@monash.edu (M.C. Thompson).

https://doi.org/10.1016/j.tsep.2022.101242
Received 24 August 2021; Received in revised form 12 February 2022; Accepted 13 February 2022
Available online 23 March 2022

a viscous term by Brinkmann [8]. However, Brinkman did not take into consideration both the boundary and the inertial effects simultaneously. Furthermore, the last stage can be identified by the model established by Wooding [9], where the convective inertia term in the divergence form was added to the Darcy equation. Consequently, these stages are brought together in a single generalised momentum equation that incorporates the Forchheimer, Brinkmann, and Wooding models with the well-known Darcy equation, referred to in the literature as the Brinkman–Forchheimer-extended Darcy model. This model has become a more popular tool to investigate the momentum transport throughout porous media.

As a matter of energy transport, the essential assumption predominantly employed in modelling is that of local thermal equilibrium $(LTE)$ among both the fluid and solid phases at every instant of time. In this case, merely one energy equation is needed to simulate the thermal conduct. However, the performance of several thermal systems relies on the non-equilibrium degree between both phases. Thus, the $(LTE)$ approximation becomes invalid, therefore two energy equations, i.e. one for each phase, are needed, which are coupled by convection term. The first two-phase energy $(LTNE)$ model was derived by Schumann [10] who suggested a simple expression for accounting the non-equilibrium state for incompressible forced convective flows in porous media. The additional convective term between the two phases in the $(LTNE)$ model requires information about the particle-to-fluid convective coefficient. A large volume of research has been conducted, for instance [11–16], to formulate such coefficient in different porous beds. Also, the flowing fluid component in porous media bears sinuous tracks, and the macroscopic fluid mixing is referred to as a mechanical dispersion. Thermal characteristics are strongly influenced by this mechanism, in all directions with reference to the bulk flow. The experimental studies of [17–19] were the pioneers in this regard, besides later works done by [20–24].

Interesting, a large volume of research has been published in various fields of interest relating to convection in porous media. Worthy review articles have been reported by [1,25–32] for summarising the latest literature testifies to the ripeness of convection in porous media overall. However, the existing literature has been mostly dedicated to either forced or natural convection, and the area of combined forced and natural convection, which constitutes the interaction between these two modes, has been, by comparison, largely overlooked. In fact, there are several thermal systems are working in the mixed convection regime, for instance, heat sinks, cooling of electronic instruments, solar plants, heat exchangers, etc, see [33–35]. So, it is important as other modes of heat transfer. In mixed convection, there are two driving forces namely; buoyancy forces and forced convective flow, which are in conflict for domination. Indeed, interestingly, there is a high possibility of obtaining oscillatory convective flows (unsteady solutions) in such systems depending on the directions of the driving conflicting forces. Therefore, in order to assist out the reader in appreciating the importance of the research that has been performed about mixed convection in porous channels, an appropriate literature review was undertaken and is summarised in this article. To illustration, the studies that used Darcy model to describe the flow in mixed convection throughout a porous media will be reviewed first, and then the studies that included the non-Darcian effects. Later, the literature will describe the researches based on the use of $(LTNE)$ energy model in mixed convection to give good clarity about the shortage of using this model in mixed mode of heat transfer within the porous media.

## 2. Literature review

### 2.1. Darcian mixed convection

The studies reviewed in this section used Darcy model for calculating the flow velocity throughout porous media. As mentioned in the prior section, Darcy's law was the first and most basic empirical formulation introduced by Darcy [6]. He conducted an experimental research to study the water flow within a vertical column filled with sand and found that the flow velocity is proportional to the pressure gradient in the flow direction as follows:

$$\frac{dp}{dx} = -\frac{\mu_f}{K u_D}, \tag{1}$$

where, $(K)$ is the permeability of the porous medium, and $(u_D)$ is the Darcian fluid velocity in the $x$-direction. It cab be seen in Eq. (1) that Darcy's law does not take into consideration the flow inertia effects and the rigid wall effects existed next to the porous medium. Indeed, there is a general consensus, see for example, Palm et al. [36],Chandrasekhara and Vortmeyer [37], and Bear and Corapcioglu [38], that this model is valid only when the Reynolds number, on the basis of the particle diameter or the square root of permeability, is less than unity and becomes inadequate either at high flow rates or in a high porosity media.

The works of [39–43] were the pioneering researches that used the Darcy model to conduct earlier analyses into forced and free convection within porous media. Nevertheless, their principal attention was to test the flow instability and the determination of the circumstances that give rise to mixed convection. Combarnous and Bia [44] was one of the first studies to utilise both experimental measurement and numerical computation to examine the convection onset in a porous bed confined with two parallel impervious boards. It was assumed that the convection occurs when $(\mathrm{Ra} > \mathrm{Ra}_{crit} = 4\pi^2)$, where (Ra) is the Rayleigh number and $(\mathrm{Ra}_{crit})$ is the critical Rayleigh number. Their findings showed that neither the circumstances for the convection onset nor the relationship between Ra and $\mathrm{Ra}_{crit}$ were affected by the presence of a low flow velocity. This finding was agreed with the linear analysis of Prats [41]. By employing the formulation of boundary layer, and utilising the similarity and integral methods, Cheng and co-workers [45–49] performed many of extensive works to investigate mixed convection over horizontal, vertical, and inclined slabs. In the work of Cheng [46], Cheng obtained the similarity solutions for a specific instance when the wall temperature $(T_w = T_\infty \mp ax^n)$ and the free stream velocity $(u_\infty = bx^m)$ change in accordance with the power function of distance, where $(a)$, $(b)$, $(n)$, and $(m)$ are constants. They found that the similarity solutions subsist merely when $(n = (3m+1)/2)$. Minkowycz et al. [50] modified the work of Cheng [46] to the situation when the wall temperature varies arbitrarily based on power law for both stagnation-point and parallel flows, where acquiring similarity solutions are inaccessible. They used the local non-similarity method to obtain approximate solutions for mixed convective flows over a hot wall immersed in porous medium with wall temperature being a power function of distance. Following, Chandrasekhara [51], also developed the work of Cheng [46] to incorporate the influence of variable permeability for the same two cases. It was revealed that the variation of the permeability considerably enhances the rates of heat transfer. Later, Nakayama and Koyama [52] and Nakayama and Pop [53] obtained approximation solutions for the problem of boundary layer flow in mixed convection over walls embedded in porous media using the local similarity solution method. For example, Nakayama and Pop [53] developed an integrated similarity transformation that covering every possible similarity solution in forced, natural, or mixed convection throughout non-Darcy and Darcian porous media.

Aldoss et al. [54] reported non-similarity solutions under condition of variable heat flux (VHF) $(q_w = ax^n)$ about a horizontal wall submerged in a porous substrate utilising two different transformations, where $(a)$ and $(n)$ are constants. In first one, the non-similarity parameter $(\xi_{(force)} = \mathrm{Ra}_x \mathrm{Pe}_x^2)$ was employed, and the solution covered the system when forced convection is predominated. The second one involved the non-similarity parameter $(\xi_{(natural)} = \mathrm{Pe}_x \mathrm{Ra}_x^{1/2})$, and the solution covered the system controlled by free convection. It is to mention that $(\mathrm{Pe}_x)$ and $(\mathrm{Ra}_x)$ are the local Péclet and Rayleigh numbers, respectively. The solution of the whole mixed convection was established utilising the solutions of both systems to prevent any singularity difficulty at the limitative ends. Aldoss et al. [55] used similar technique employed by Aldoss et al. [54] to solve similar problem but with variable wall temperature (VWT) heating condition ($T_w - T_\infty = ax^n$). In this study, the non-similarity parameter ($\xi_{(force)} = \mathrm{Ra}_x \mathrm{Pe}_x^{3/2}$) was used to address the problem in the regime dominated by forced convection, and ($\xi_{(natural)} = \mathrm{Pe}_x \mathrm{Ra}_x^{2/3}$) was employed covering the regime dominated by free convection. In both studies Aldoss et al. [54,55], two non-similarity parameters were employed for each heating case, and basic correlations for local and average Nusselt numbers were formulated for the whole mixed convection regime. After that, once again the same authors Aldoss et al. [56] solved the same problem treated by Aldoss et al. [54,55] using also similar technique but this time to obtain a single non-similarity parameter that covers the overall regime of combined natural and forced convection. They solved the problem for the two heating cases, (VHF) and (VWT). The single non-similarity parameter for the case of (VHF) was ($\chi^*_{(x)} = 1/\left(1 + (\mathrm{Ra}^*_x \mathrm{Pe}_x^2)^{1/4}\right)$), whereas the another parameter for the case of (VWT) was ($\chi'_{(x)} = 1/\left(1 + (\mathrm{Ra}_x \mathrm{Pe}_x^{3/2})^{1/3}\right)$). It was found that both cases have the same temperature profiles, in relation to the variations of the velocity and temperature gradients, as well as the variation of the thermal boundary layer thickness at the surface relating to non-similarity parameters.

All solutions that have been found in all previous aforementioned studies have been dependent on the boundary layer theory using the Darcy model. Considering the full Darcy equation, there have been comprehensive numerical works to investigate the effects of buoyancy forces on the forced flow throughout horizontal porous channels. Haajizadeh and Tien [57] considered the case where the forced flow and the temperature gradient are introduced in the same horizontal direction. Thus, the buoyancy-driven movement is due to the temperature difference between the channel ends, while the forced flow is caused by the pressure gradient at the channel ends. They examined numerically and analytically the influence of the following non-dimensional parameters: Rayleigh number, Péclet number, and the aspect ratio of the channel (length/height). It was shown that there is a non-linear interaction between the forced flow and the thermally driven motion through the channel, affecting the velocity and temperature fields. However, the heat transfer augmentation owing to the contributions of these two forces might be summed together. It was also shown that even small values of Péclet number can considerably redistribute the temperature within the canal, and high values of it suppress significantly the free convection. Hence, a linear behaviour for the temperature with negligible dependence on the vertical position were obtained.

By contrast, [58–60] studied the case where these two driving forces are perpendicular to each other. Thus, the through-flow is in the horizontal direction and the buoyant flow is imposed in the vertical direction by a localised heater positioned on the lower wall, for various thermal boundary conditions. For instance, Lai et al. [58] considered the thermal boundary condition when both the upper and lower walls are isothermally cooled. They investigated the steady-state mixed convection for different Rayleigh and Péclet numbers when the heater length is similar to the porous layer thickness, e.g. ($L_h/H_p = 1$). The results revealed that for small Péclet numbers, the entire channel is dominant by the buoyancy effects, generating two symmetric recirculating vortices close to the heater edges. The temperature distribution was also found to be approximately symmetric around the centre line of the heater, as shown in Fig. 1a. However, as Péclet number increases, see Figs. 1b and 1c, the symmetry nature of the thermal field deforms, and the intensity of the vortices decreases, demonstrating the commencing of the forced convection dominance.

Different to the case of Lai et al. [58,59] considered another thermal boundary condition, which is the top surface of the channel is isothermally cooled, while the bottom surface is assumed to being insulated unless the heated section. They also investigated the steady-state case of mixed convection. They examined the effect a heater length ($A = L_h/H_p = 0.5-5$) on the velocity configuration, temperature distribution, and rates of energy transport, for variant Rayleigh and Péclet numbers. They reported that at low Rayleigh numbers, changing the size of heat source does not influence the thermal field, and produces basically similar bi-cellular flow behaviours, as illustrated in Fig. 2. However, at large Rayleigh numbers, recirculating multi-cells were developed, but the transition from a multi-cellular flow into a bi-cellular flow was noticed to be reliant on Péclet number, as displayed in Fig. 3, which is similar to that observed by Lai et al. [58]. Prasad et al. [60] considered the same problem and thermal boundary condition of Lai et al. [59], which is top horizontal wall isothermally cooled with adiabatic bottom wall containing a finite isothermal heater, but this time for a heater length of ($L_h/H_p = 1$), similar to that assumed by Lai et al. [58]. The results showed similar bi-cellular flow reported by Lai et al. [58], and displayed in Fig. 1a, for two pairs of rotating cells generated near the heater at low Péclet number and high Rayleigh number.

Mixed convection heat transfer from a flat plate immersed in a porous layer located near and under an insulated flat surface, demonstrated in Fig. 4, was numerically examined by Oosthuizen [61]. The plate was heated to a uniform temperature, which is higher than the temperature of the flowing fluid. Solutions were obtained for values of the forced flow parameter Péclet number (Pe = 0 and 300), the buoyancy parameter $(\mathrm{Ra}^*\mathrm{Pe} = 0 \text{ and } 8)$, where ($\mathrm{Ra}^*$) is the Darcy–Rayleigh number, and the depth of plate below surface ($H_p$ = 0.25, 0.35, 0.5, and 0.5). It was indicated that when the buoyancy effects are neglected, the impact of the impermeable adiabatic surface on the heat transfer rates become negligible at ($\mathrm{Pe} > 2H_p^2$), whereas in the combined convection region, the presence of the surface causes a significant increase in the rate of heat transport on the upper surface of the plate. The results also clarified that the mean Nusselt number varies linearly with the buoyancy parameter for any given values of (Pe and $H_p$) in the mixed convection region.

Lai et al. [62] investigated numerically unsteady natural and combined convection within a flat porous layer heated from the bottom by multiple, isothermal, discrete heat sources. The disconnected heat sources are assumed to have the same length and are separated from each other by a constant interval. It was noted that, for free convection or for mixed convection at small Péclet numbers, the flow and temperature fields for a long single heater are very similar to those for multiple heaters. For example, their free convective flow behaviour for two heaters of ($L_h/H_p = 1$) at (Ra=100) is similar to the mixed convective flow for long heater ($L_h/H_p = 3$) at low Péclet number (Pe=0.1) and high Rayleigh number (Ra=100) reported by Lai et al. [59], see the comparison in Fig. 5. However, as Péclet number increases, the flow structure and the variation of local Nusselt number for these two cases are entirely different. For a single heat source, the heat rejected to the top wall is mainly by the first inner cell, and the second cell has a less contribution. However, for the multiple sources, the internal cells have equal contribution to the heat transferred. Another interesting finding, which was not observed and reported by previous studies of [58–60], is that oscillatory flows are developed causing unstable thermal fields at Péclet number (Pe = 5) and Rayleigh number (Ra = 100). This is owing to the instability of the thermal boundary layer resulted from the repeated thermal disturbance caused by the preceding source. Similar oscillatory flows were also reported by Lai and Kulacki [63] and Lai and Kulacki [64] when considering a long single heater. They reported that this instability of the hydrodynamic field is owing to the demolition and restoration processes of the flow recirculation, and the period of the oscillation is found to be a function of Péclet number.

Experimental study was conducted by Lai and Kulacki [65] for the same problem described by Prasad et al. [60], but this time for natural and combined convection inside a horizontal bed packed with glass spheres under a heating action from the bottom by a localised heat element. They used (3 mm) diameter spheres saturated by water as a working fluid, and considering three various sizes of heat source ((source length)(layer depth) = ($L_h H_p$) = 1,3, and 5). For mixed convection, the experimental results were obtained for Péclet number

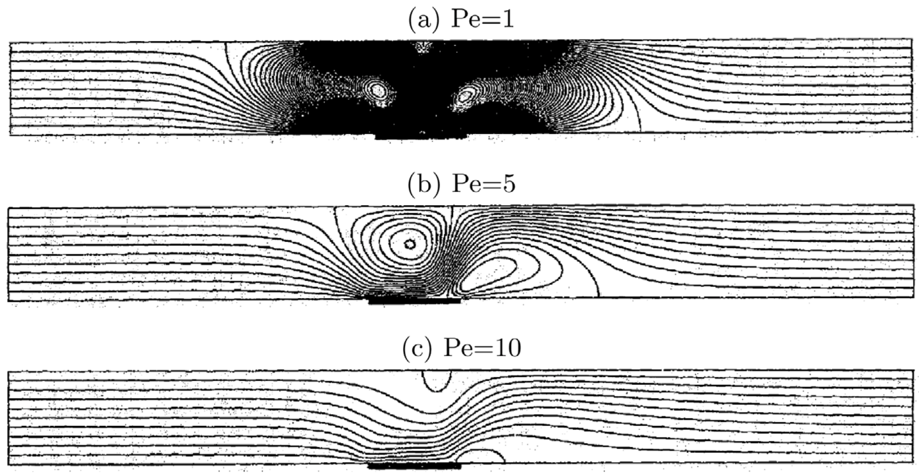


**Fig. 1.** Results of Lai et al. [58] for the influence of Péclet number (Pe) of (a) 1, (b) 5, (c) 10, on the flow field in a porous channel heated from below by a heater of size ($L_h/H_p = 1$), at Ra=100.

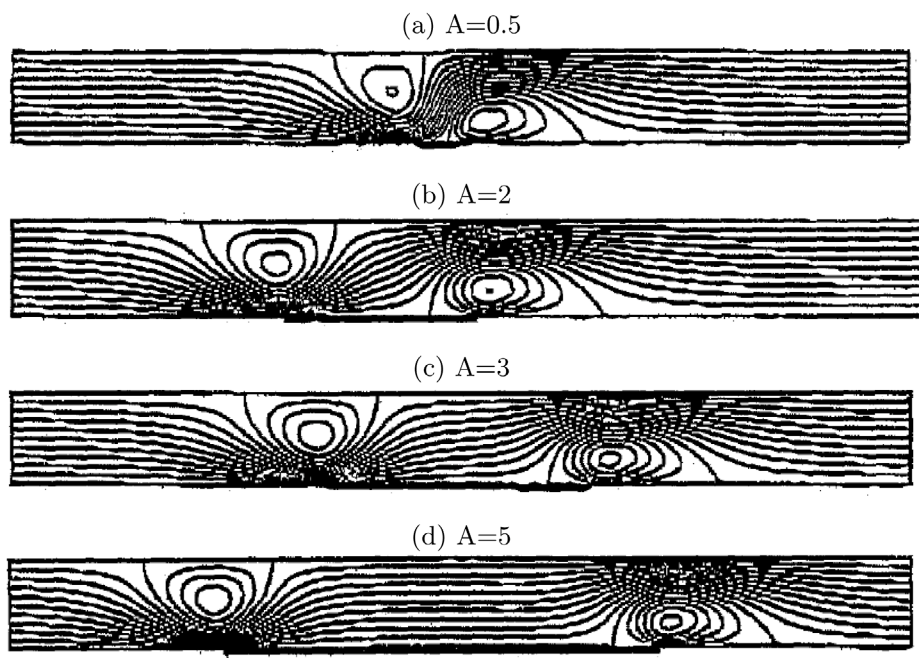


**Fig. 2.** Results of Lai et al. [59] for the effect of heater size ($A = L_h/H_p$) of (a) 0.5, (b) 2, (c) 3, (d) 5, on the flow behaviour within a porous channel heated from below at Ra=10 and Pe=0.5.

(Pe = 0.1 – 120) and Rayleigh number (Ra = 1 – 1000). It was found that there is almost a (10%) discrepancy between the experimental data and published predicted data as a result of the inappropriate incorporation the thermal conductivity in the energy equation. Hence, by using the effective thermal conductivity, an excellent agreement is achieved between these two results. In addition, at ($L_h H_p = 3$ and 5), the flow was noticed experimentally to become oscillatory owing to the thermal boundary layer instability. This instability is as a result of the strong interact between the external-induced flow which tries to suppress the thermal boundary layer and buoyancy effects that attempt to thicken it. Indeed, Prasad et al. [60] did not report this flow behaviour numerically as they solved the steady-state governing equations; however, Lai et al. [62] and Lai and Kulacki [63,64] who solved numerically the transient Darcy' law, predicted such oscillating flows in horizontal porous channels.

It is well established in the literature that the flow and heat transfer characteristics of laminar forced convection channel flows are significantly affected by the buoyancy-induced secondary flow inside rectangular ducts. Chao and Hwang [66] examined the buoyancy-induced secondary flow coupled with a forced axial flow in a horizontal Darcian rectangular duct displayed in Fig. 6. The duct was assumed to be under a uniform temperature peripherally and subjected to an axially uniform heat flux. The study was performed for a wide range of duct aspect ratio ($0.01 \le AR =$ (width height) $\le 100$) and Darcy–Rayleigh number ($0 \le$ Ra $\le 10^4$). They predicted dual solutions between two-cell and four-cell flow configurations at variant Darcy–Rayleigh numbers and duct aspect ratios. But, the interesting one that was found at very width-narrow duct at ($AR = 0.1$ and 0.01), at (Ra $= 5 \times 10^3$). This multiplicity flow behaviour was observed experimentally by Buretla and Berman [67], and numerically by Islam and Nandakumar [68] who employed Brinkman–Darcy model in a square duct. They presumed that it might be a bifurcation phenomenon. It was also found that when ($AR \to \infty$), the effect of vertical side walls becomes negligible. Thus, the hydrodynamic and thermal characteristics in the core region of the rectangular channel with large values of ($AR$) are expected to be similar to that of parallel plate

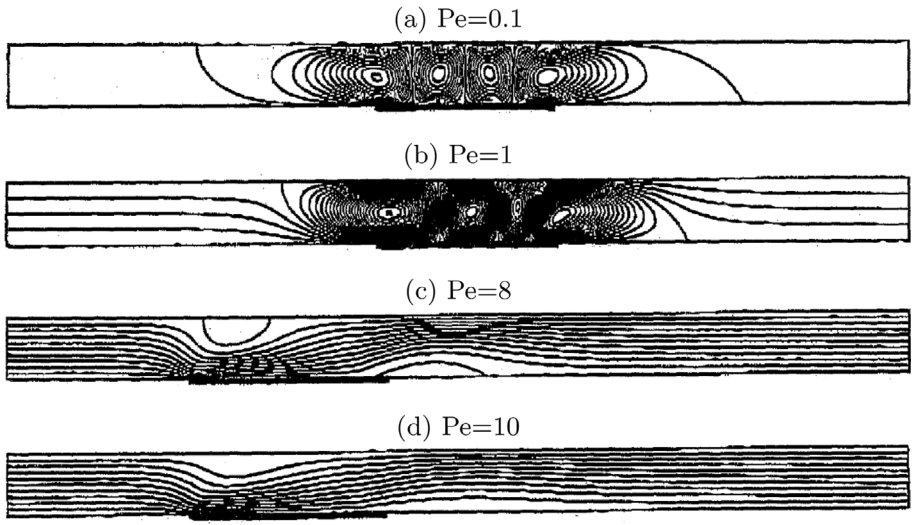


**Fig. 3.** Results of Lai et al. [59] for the effect of Péclet number (Pe), from top to bottom (*a*) 0.1, (*b*) 1, (*c*) 8, (*d*) 10, on the flow field inside a porous channel containing a heater with size of ($L_h = 3 \times H_p$) at the bottom, at Ra=100.

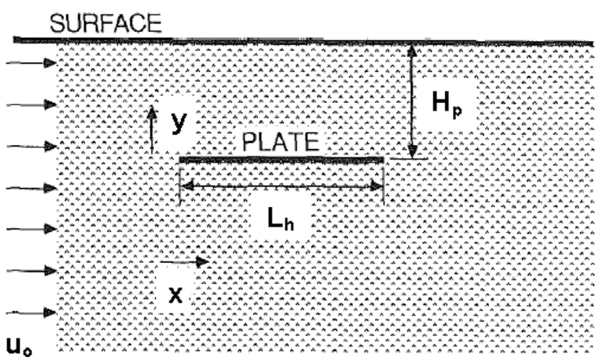


**Fig. 4.** The physical problem considered by Oosthuizen [61]. (Replotted).

channel. Therefore, there should be a relationship between the onset of the rotating eddies in the central region of the rectangular channels and horizontal plates. Chao and Hwang [69] investigated numerically mixed convection in a rectangular horizontal porous channel of aspect ratio (5) under five various circumferential heating conditions. In these five cases, an axially uniform heat flux and heat input on different side walls are subjected, and the temperature of the heating wall is circumferentially uniform but varies linearly in the axial direction. The porous material is made of fine sintering copper beads of diameter ($d_p$ = 0.072 mm), and the water flow is very slow (Re < 1) even the Darcy flow model to be valid. The results demonstrated that the strength and pattern of buoyancy-induced secondary flow are also significantly sensitive to the circumferentially distribution of wall heat flux. It was seen that the intensity of secondary flow and enhancement of heat transfer in case of heating the channel from below with insulation from above are stronger than that in the case of heating of top wall with adiabatic bottom wall regardless of side wall heating conditions.

Saeid and Pop [70] considered similar physical problem deemed by Lai et al. [59] and Prasad et al. [60], which is mixed convection in a porous layer bounded by double horizontal walls, warmed from the bottom. Also, similarly, the bottom wall is adiabatic, except the heat source, while the upper wall is considered to be cooled isothermally. However, Saeid and Pop [70] investigated the unsteady case of the problem and for different heating condition, which is at fixed heat flux. The average Nusselt number ($Nu_m$) was calculated for a particular case of Rayleigh number (Ra = $10^2$), but for variant values of Péclet number (Pe = $0.1-10$) and heater length ($L_h/H_p = 1, 3$, and 5), where ($L_h/H_p$) represents the ratio of heater length to the porous layer thickness. As predicted previously by Lai et al. [58,59],Prasad et al. [60],Lai et al. [62], and Lai and Kulacki [63,64,65], the results showed that when Péclet number is low, the mode of natural convection dominates the system; however, for high Péclet numbers, the mode of forced convection becomes the dominant. Whereas, for temperate values of Péclet number, it was seen that oscillatory mixed convective flows take place for the heater lengths of ($L_h/H_p$ = 3 and 5), and accordingly Nusselt number was shown to vary periodically with the time, as demonstrated in Fig. 7. Indeed, these oscillations, which were also observed in the works of Lai et al. [62] and Lai and Kulacki [63,64,65], represent the equilibrium status between the external flow effects and the buoyancy effects.

In another study, Saeid and Mohamad [71] took into consideration the buoyancy effects to research in the regime of mixed convection, but this time in jet impingement cooling of a horizontal saturated porous layer under the heating effect from the bottom by a finite isothermal heat source, as displayed in Fig. 8. They presented results for the effects of the following parameters: Péclet number ($1 \leq Pe \leq 1000$), Rayleigh number ($10 \leq Ra \leq 100$), dimensionless jet width ($0.1 \leq d/L_h \leq 0.9$), dimensionless porous layer thickness ($0.1 \leq H_p/L_h \leq 1.0$), where, ($L_h$) is a half length of the heat source. Their results indicated that when Péclet number is high, the increase in either jet width or Rayleigh number raises the mean Nusselt number. They also concluded that when the space between the heated part and the jet hole decreases, the convection heat transfer might be enhanced. Furthermore, once again that similar to Lai et al. [62],Lai and Kulacki [63,64,65] and Saeid and Pop [70], they could not obtain steady-state solutions for the same flow circumstances when the buoyant flow and the exterior jet flow are in challenge for the dominance. Instead, oscillatory convection without reaching the steady state was found for these cases, as demonstrated in Fig. 9.

Sivasamy et al. [72] repeated the same study of Saeid and Mohamad [71] to investigate the thermal performing of mixed convective cooling jet impinging a heat element immersed in a horizontal porous canal, but this time under constant heat flux heating. They tested the impact of the buoyancy forces of the thermal performance for the following main parameters: Rayleigh number (Ra = 10 – 100), Péclet number (Pe = 1 – 1000), jet width ($d/L_h$ = 0.2 – 2.0), and the thickness of the porous layer ($H_p$ = 0.1 – 1.0). Once again, the same conclusions found by Saeid and Mohamad [71], were reported. Thus, for high Péclet number, the mean Nusselt number enhances with an increase in either the jet width or Rayleigh number. However, the mean Nusselt

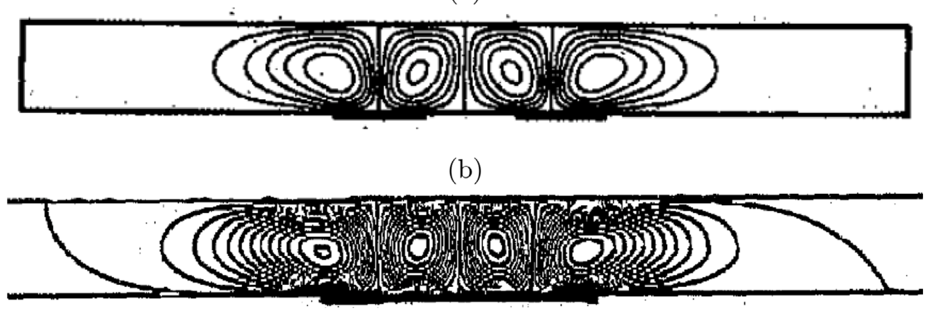


**Fig. 5.** (a) Free convective flow field within a porous canal containing two discrete heaters at the bottom, at Ra=100 reported by Lai et al. [62], and (b) mixed convective flow field above a single long heater ($L_h/H_p = 3$) at low Pe=0.1 and high Ra=100 reported by Lai et al. [59].

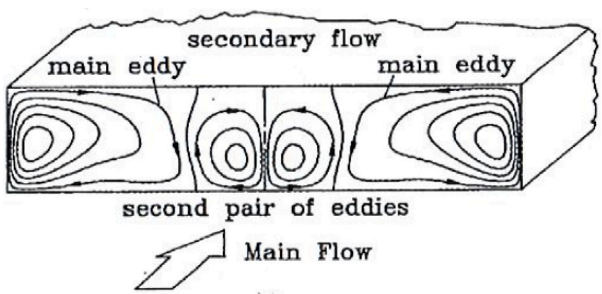


**Fig. 6.** The physical configuration of a rectangular duct studied by Chao and Hwang [66].

number was found to enhance as the porous layer thickness decreases. It was also found that the counteraction of buoyancy driven flow versus the jet flow in mixed convection mode causes unfavourable minimum Nusselt numbers. But, interestingly, their results did show oscillatory convective conduct as was found by Saeid and Mohamad [71], although the transient governing equations were considered, see Fig. 10.

Saeid [73] studied conjugate heat transfer and opposing mixed (free-forced) convective flows generated due to injecting a fluid perpendicularly for cooling a rectangular thick solid wall, heated from below and submerged inside a horizontal porous layer, as shown in Fig. 11. He investigated the influences of wall thickness ($H_w/L_h = 0.1-0.5$), jet width ($d/L_h = 0.1-0.5$), and solid-to-porous thermal conductivity ratio ($K_r = (k_w/k_p) = 0.1 - 10$), for different Péclet and Rayleigh numbers, (Pe $= 1 - 1000$) and (Ra $\leq 100$), respectively. A set of momentum and energy steady equations was used to compute the flow and thermal fields, therefore, the ability of capturing the features of the oscillatory mixed convective flows was not possible, as captured by Lai and Kulacki [64],Saeid and Pop [70], and Saeid and Mohamad [71] for the same problem. It was reported that for low Péclet numbers, e.g. when the free convection is dominated, a heat transfer enhancement can be obtained by raising whether Rayleigh number or the thermal conductivity of the solid wall, and/or by reducing the solid wall thickness. However, for high Péclet numbers, e.g. when the forced convection is dominated, it was predicted that the improvement in heat transfer might be achieved by raising either Péclet number, solid wall thermal conductivity or jet width, and/or by lessening the thickness of the solid wall. Therefore, the study recommended that for an effective cooling to be acquired, thinner solid wall with higher thermal conductivity should be considered, as well as by eschewing to work in the opposing mixed convection regime as much as possible.

Sphaier and Barletta [74] and Barletta et al. [75] reported a linear stability analysis for a mixed convective flow inside a horizontal porous canal. Sphaier and Barletta [74] considered a 2-$D$ plane porous stratum bounded by double solid walls; the lower wall is heated form below with a fixed heat flux and the top one is adiabatic. Whereas, Barletta et al. [75] investigated the flow instability within a 3-$D$ horizontal rectangular porous channel having an iso-flux lower plane and imperfectly conducting upper plane, while the side-planes are assumed to be insulated. Their analyses were performed using the Darcy model and the perturbation solution for global oblique rolls, resulting to an eigenvalue problem. The eigenvalue problem was solved by implementing a hybrid numerical–analytical technique for defining critical values of Darcy–Rayleigh number in terms of the perturbation angular frequency, Péclet number, and wavenumber. The results of the first study revealed that for oblique rolls, all nonzero angular frequency values cause unstable flow; however, for longitudinal rolls, the only zero value of the angular frequency was found to cause the flow instability. Whereas, the results of the second study demonstrated the transition conditions to the convective instability, and then to the absolute instability for small amplitudes. It was reported that the transition to the convective instability is vigorously sensible to Biot number, and the transition to the absolute instability occurs with 2-$D$ perturbations.

Ozgen and Varol [76] studied steady-state mixed convection in the same physical configuration considered by Lai et al. [59] and Prasad et al. [60], which is a porous layer bounded by two horizontal walls, heated from the bottom by a localised heater. Additionally, likewise, the lower wall is adiabatic, excepting the heater, whereas the upper wall is isothermally cooled. However, Ozgen and Varol [76] examined the problem for different configuration dimensions. Thus, the channel length was assumed to be ten times greater than the channel height ($L_c = 10H_c$), while the length of heat source was considered to be 1/3 of the channel length ($L_h = L_c/3$). They characterised the influence of Péclet number (Pe $= 0.5 - 5$) and Rayleigh number (Ra $= 100 - 1000$) on Nusselt number and the flow behaviour. In spite of the fact that the steady-state of Darcian model was employed, they claimed that their results confirmed forming oscillatory flows for a short time at low Péclet number (Pe $= 0.5$), after which the flow reaches the steady state condition. However, at (Pe $= 1.0$), continuous periodic flows were observed in the channel without reaching the steady state, for different Rayleigh numbers. Indeed, their results did not show these periodic cases. Instead, similar to what was revealed by Lai et al. [59] and Prasad et al. [60], stable flow and temperature patterns were reported, as illustrated for example in Fig. 12 at Péclet number (Pe $= 1.0$) showing the transition into the multi-cellular flow as Rayleigh number increases from 100 to 1000.

Aiding and opposing flows, whether adjacent to a heated vertical surface or bounded by two vertical plates in fully developed region using the Darcy flow model, have been the topic for many works. Parang and Keyhani [77] investigated a buoyancy-assisted mixed convective flow in an annular filled with a porous material experiencing a regular heating from outer and/or inner wall. Lai et al. [78] studied the conflict between a downward or an upward through-flow and a buoyant flow stimulated by a short heater positioned on the left bounding surface of a two-dimensional vertical porous layer. The left surface is considered insulated except the heat element, while the right surface is

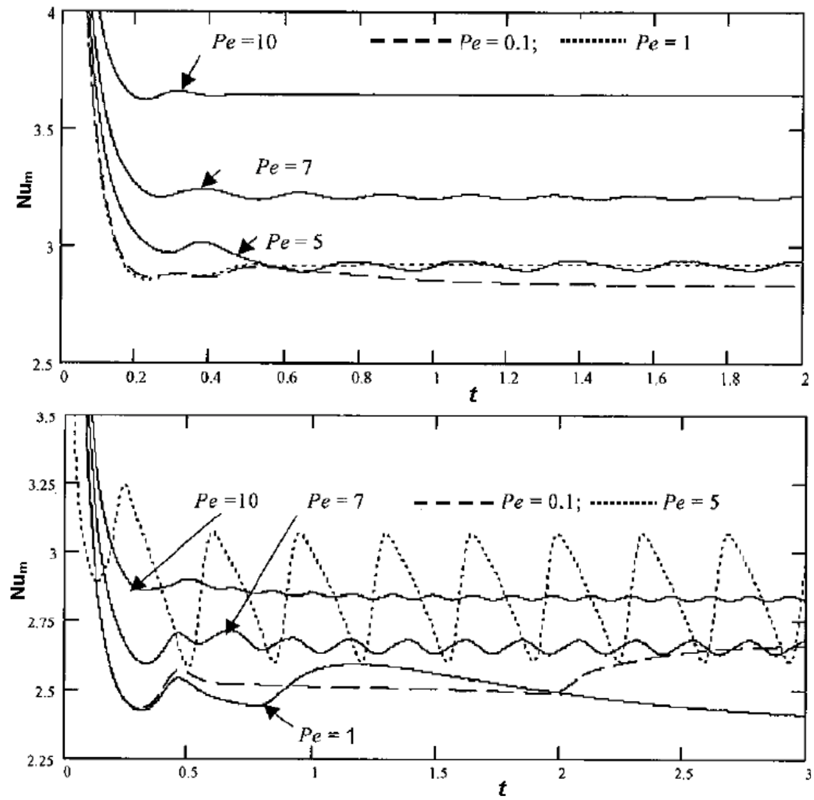


**Fig. 7.** Variation of average Nusselt number ($Nu_m$) with time ($t$), for different Péclet number, and at Rayleigh number Ra=100, and for two heater sizes; $L_h/H_p$=3 (Top) and $L_h/H_p$=5 (Bottom), presented by Saeid and Pop [70]. (Replotted).

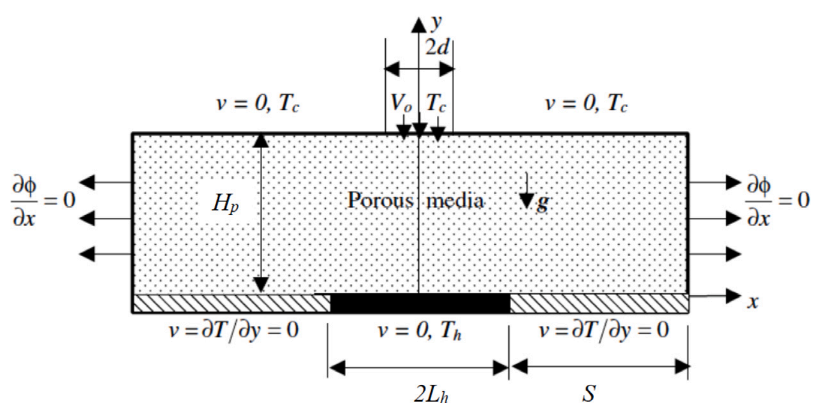


**Fig. 8.** The physical domain of cooling jet impinging a heat element immersed in a horizontal porous layer, Saeid and Mohamad [71]. (Replotted).

isothermally cooled, and the heater length is assumed to equal the channel height. The numerical results revealed that when the mode of mixed convection begins, the primary fluid flow separates from the perpendicular surface, reattaches afterward producing a steady recirculated subsidiary flow within the annulus. In the case of aiding flow, separation and reattachment occur on the coldish surface, also the convective cell broadens apart from the heater. The rates of heat transfer were shown to be augmented with Péclet number in such assisting flow case. Nevertheless, during the counter flow, the recirculation takes place on the warmed surface, and the extent and the strength of the convective vortex significantly rely on the values of Rayleigh and Péclet numbers. Interestingly, it was reported that the rates of heat transfer at lower Rayleigh numbers might be bigger than that at higher Rayleigh numbers under particular conditions. Pop et al. [79] examined theoretically this communication between the forced and buoyant flows, but inside a vertical of narrow channel stuffed with a porous substrate. The boundaries were maintained at identical ambient temperatures with the exception of local heating source on the left wall. It was predicted that there are certain values of mixed convection parameter and duct width that have serious effects on generating recirculating flows within the domain. For instance, regions of such reversed flows were observed at the mixed convection parameter equals to 2.5 and smaller duct width.

In the another work, with two iso-flux heat sources located on the adiabatic left surface, Saeid and Pop [80] examined a stabilised mixed convective flow in a parallel plate columnar channel immersed in a porous material. The results were generated to show the effect of the segregation space between the heat sources ($L_d$), the lengths of heaters ($L_{h1}$ and $L_{h2}$), the ratio of their heat fluxes ($q_1 q_2$), as well as the external flow configuration. For aiding flows, the results referred to the independency of thermal dissipation on the bottom heater; however, the thermal dissipation from the top one is significantly influenced by

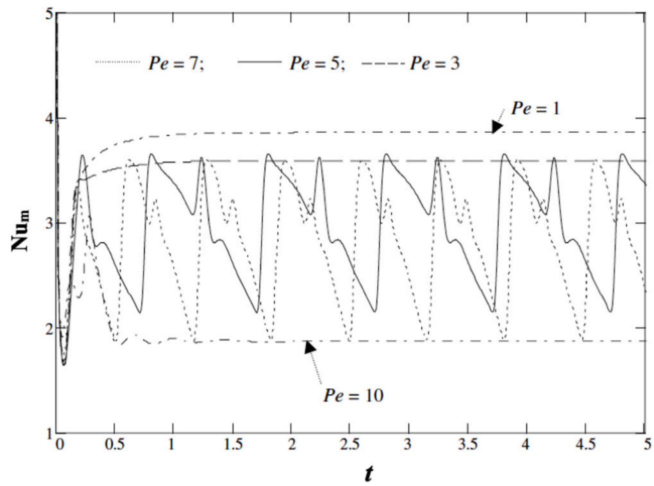


**Fig. 9.** Variation of temporal Nusselt number for different Péclet number, at Rayleigh number Ra=100, jet width $d/L_h$=0.9 and porous layer thickness $H_p/L_h$=1, reported by Saeid and Mohamad [71]. (Replotted).

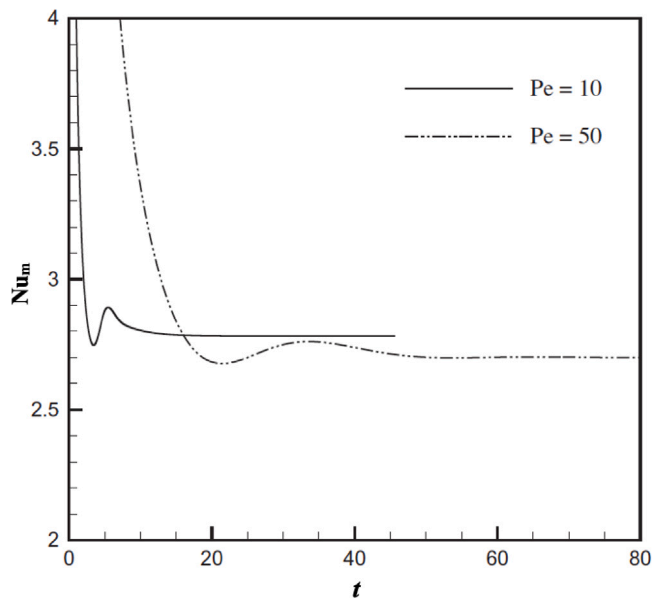


**Fig. 10.** Variation of temporal Nusselt number for Péclet number Pe=10 and 50, at Rayleigh number Ra=100, jet width $d/L_h$=0.1 and porous layer thickness $H_p/L_h$=1, reported by Sivasamy et al. [72]. (Replotted).

the existing of the bottom heater. It was also shown that for opposing flow, the mean Nusselt number over the bottom heater enhances as the separation distance between the heaters ($L_d$) increases or as either the flux ratio ($q_1 q_2$) or the length of top heater ($L_{h1}$) decreases. Similar phenomenon was also investigated by Mahmud and Pop [81], but this time in a vertical square vented cavity packed with a porous medium. It was assumed that the forced flow is imposed to enter the cavity throughout an inlet port and exit it via a vent, while the natural convection was considered by heating one of the perpendicular walls and the residual surfaces are kept adiabatic. The obtained findings showed that the total heat dissipation from the cavity depends strongly on the ratio of vent width to the cavity height, for fixed values of the Rayleigh and Péclet numbers. Cimpean et al. [82] presented analytical analysis of steady mixed convective flows within inclined parallel long walls stuffed with a porous medium, under a uniform heat flux on both of them. The analytical flow and thermal results were reported on the basis of Péclet number, mixed convection parameter, and the inclination angle. They found that the influence of channel inclination is strongly dependent on the value of Péclet number. Thus, for high Péclet numbers, the inclination impact is reduced, and the solution tends to be more symmetric or similar to the solution in the vertical channel.

Barletta [83] and Barletta and Celli [84] used similar stability analysis carried out by Sphaier and Barletta [74] Barletta et al. [75] for horizontal convective flows, employing Darcy's law, perturbation solution, and hybrid numerical–analytical technique, to analyse the linear stability of vertical convective flows. Barletta [83] investigated buoyancy-assisted and buoyancy-opposed mixed convective flows throughout a perpendicular porous canal, whereas Barletta and Celli [84] repeated the investigation inside an inclined porous canal. Their analyses were made for small-amplitude perturbations, and under the action of different symmetric and uniform cooling/heating circumstances. Later, Barletta and Miklavčič [85] extended the work of Barletta [83] by taking the effects of viscous dissipation into account together with the thermal buoyancy effects to analyse the nonlinear instability of dissipation-provoked dual mixed convection flows inside an upright channel.

Celik and Mobedi [86] investigated numerically and analytically the hydrodynamic and thermal domains in a vertical duct partly stuffed with a porous substance subjected to aided-buoyancy mixed convective flows. The investigation was performed for different governing parameters namely; Darcy number, Grashof number, thermal conductivity ratio, and the porous layer thickness. They reported that the opportunity of getting descending flows within the porous stratum rises by increasing the effective thermal conductivity or by reducing the thickness of porous stratum. Interestingly, the pressure drop along the channel was shown to be considerably influenced by the thermal conductivity ratio. Thus, Fig. 13 shows the variation of the dimensionless pressure gradient ($\Gamma$) with the Grashof/Reynolds (Gr/Re) parameter, at two thermal conductivity ratios ($K$ = 0.05 and 100) and two values of Darcy number (Da = $10^{-3}$ and $10^{-4}$). The figure demonstrates that as the thermal conductivity ratio increases inside the channel, the pressure drop increases greatly, especially for low Darcy numbers.

### 2.2. Non-Darcy mixed convection

The deviations from the Darcy regime by introducing the inertial and wall viscous forces are generally referred to as the non-Darcian effects. In many applications, for instance packed bed catalytic reactors, the porous medium is bounded, the fluid velocity is high and the porosity is variable; thus, it is significant for these effects to be involved in the problem. Large number of research studies has been reported on the impact of non-Darcian effects on the hydrodynamic and thermal behaviour for various media configurations. One of the first pioneering attempts to analyse their influence on convection heat transfer was carried out by Vafai and Tien [87] for forced convective flow during a porous substance confined by a parallel isothermal surface in a fixed porosity media. They applied the local volume-averaging method to establish the macroscopic governing momentum and energy equations that account for these effects.

#### 2.2.1. Darcy–Forchheimer mixed convection

The first deviation comes from the tortuous path between solid particles in porous media, described in Fig. 14. This produces acceleration and deceleration of the fluid flow on the scale of a representative pore length, as well as microscopic separation of the flow, and then changes the flow inertia. This effect, which was first introduced to Darcy's formulation by Forchheimer [7] and derived later by Ergun [88] as a velocity-squared term $\left(\frac{\rho_f F}{K}\left|u_D\right|u_D\right)$, is called the "Forchheimer term" or the "inertia term". They developed the Darcy–Forchheimer model as follows:

$$\frac{dp}{dx} = -\frac{\mu_f}{K u_D} + \left(\frac{\rho_f F}{K}\right)\left|u_D\right|u_D, \tag{2}$$

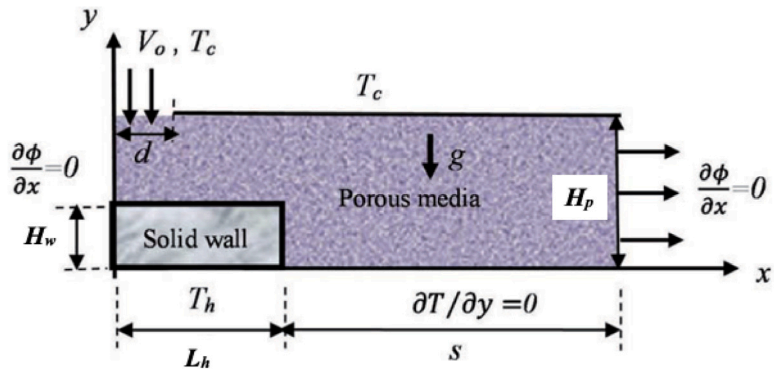


**Fig. 11.** The physical model considered by Saeid [73] to investigate opposing mixed (free-forced) convective flows generated due to injecting vertically (from top to bottom) a fluid to cool a rectangular solid wall heated from below and submerged within a horizontal porous layer. (Replotted).

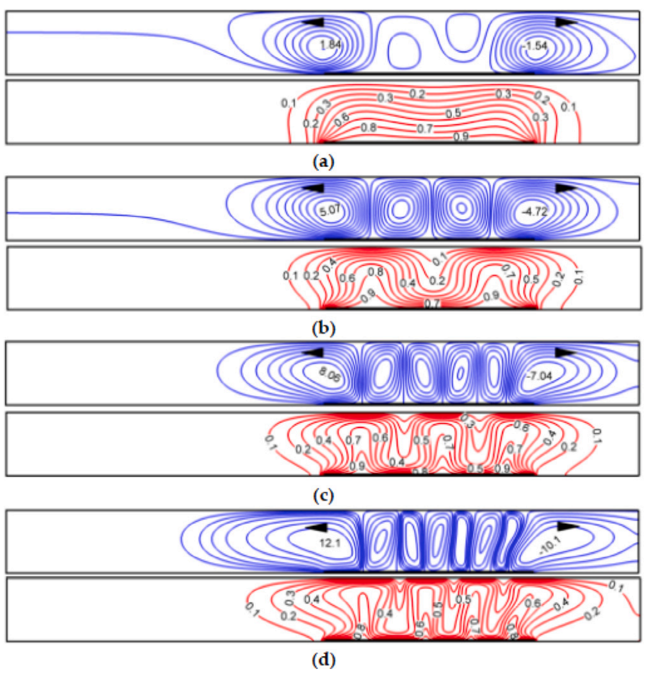


**Fig. 12.** Results of Ozgen and Varol [76] for flow and temperature patterns at Péclet number Pe=1.0, and for different Rayleigh numbers (a) Ra=100, (b) Ra=250, (c) Ra=500, and (d) Ra=1000.

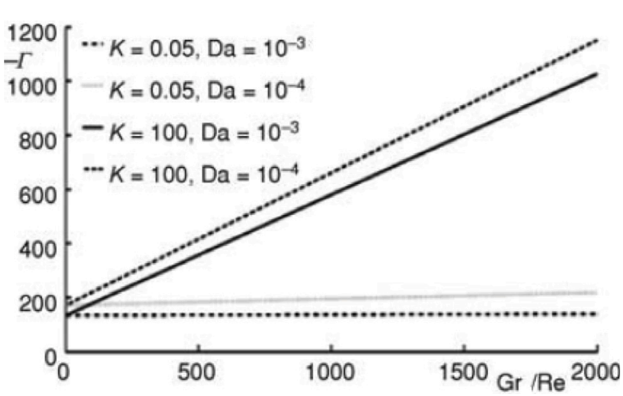


**Fig. 13.** Variation of pressure drop with (Gr/Re) parameter for different conductivity ratios ($K$) and Darcy numbers (Da). This figure was presented by Celik and Mobedi [86].

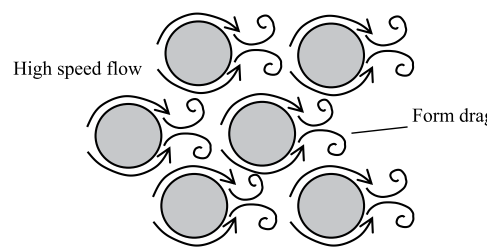


**Fig. 14.** Tortuous path for fluid flow between solid particles in porous media.

where, ($F$) is a geometry function. This model takes into consideration the creeping nonlinearity into the fluid movement, which is ascribed to the enhanced inertial resistance by the reason of the solid structure. Therefore, it is anticipated to be significant in media with high-porosity, for fluids with lower viscosity, or more particularly when convective heat transfer is existed.

Studying mixed convection in porous materials using Darcy–Forchheimer flow model, Lai and Kulacki [89] presented similarity solutions for flows during two horizontal impermeable plates under persistent wall heat flux. On the other hand, Kodah and Al-Gasem [90] investigated the effects of inertia flow, non-similarity parameter, and heating boundary conditions on the flow and heat transfer over a vertical plate. The plate is subjected to a power-law variation in wall heat flux and submersed in a saturated porous substrate. They utilised the boundary-layer formulation of Darcy–Forchheimer model and the non-similar transformation to solve the problem. It was concluded that there is a positive impact of the exponent of the power law form of heating wall conditions on the flow field through the boundary layer and intensifies the rate of heat transfer. However, the lower rates of heat transport are resulted at larger value of inertia forced effect, which reduces the velocity and broaden the temperature distribution within the boundary layer.

Islam and Nandakumar [91] analysed the problem in a fully-developed saturated porous duct of square cross-section in a horizontal orientation with peripheral condition of non-uniform heat flux with top-insulated and bottom-heated condition. The numerical simulations were carried out at a constant channel aspect ratio ($AR = 1$), and for various Grashof number (Gr = up to 12000), axial flow parameter ($\Gamma = 1$ and 30) (i.e., dimensionless axial pressure gradient), inertia parameter ($\zeta = 0 - 0.05$) and Prandtl number (Pr = 0.73, 5, 50). The results indicated that when the inertia parameter goes to zero ($\zeta \rightarrow 0$), the role of the axial flow parameter becomes simple. In such case, Darcy model is retrieved, and the duty of the axial flow parameter is only used for scaling the axial velocity. But, when ($\zeta > 0$), the Forchheimer part is recovered, and the axial velocity becomes connected to the secondary velocities within the channel. This is obvious in Fig. 15,

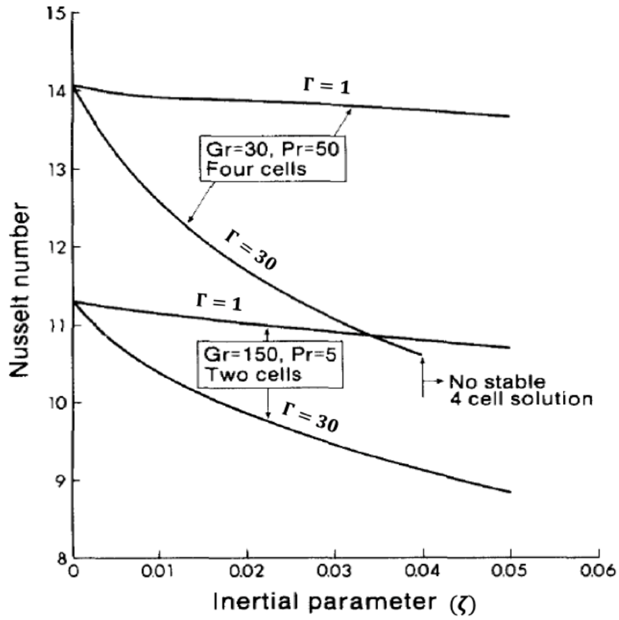


**Fig. 15.** Results of Islam and Nandakumar [91] for the variation of Nusselt number versus inertia parameter ($\zeta$) for different Gr, Pr, and axial flow parameter ($\Gamma$). (Replotted).

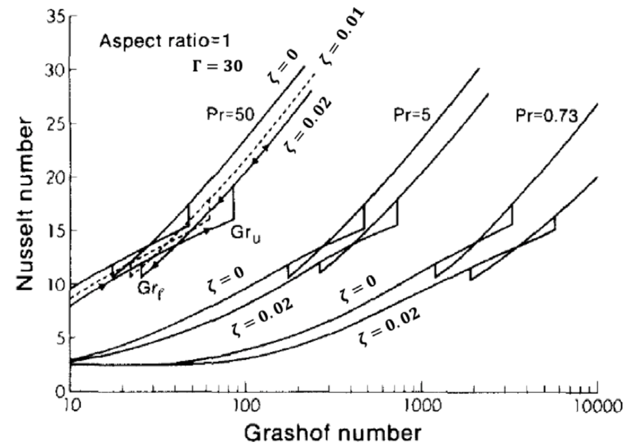


**Fig. 16.** Results of Islam and Nandakumar [91] for the variation of Nusselt number versus Gr for different Pr and $\zeta$ at $\Gamma$=30. (Replotted).

which illustrates that at ($\zeta = 0$), similar values of Nusselt number are acquired at two various values of axil flow parameters ($\Gamma = 1$ and 30). The figure displays that changing the axial flow parameter varies considerably the value of Nusselt number, which is an evidence on the importance of the inertial effect. However, changing the axial flow parameter does not alter the structure of the secondary flows generated inside the channel as other parameters such as Grashof and Prandtl numbers do. In addition, the results exhibited dual solutions and hysteresis behaviour over a certain range of Grashof number. It was shown, as illustrated in Fig. 16, that the variation of lower critical Grashof number ($Gr_l$) and upper critical Grashof number ($Gr_u$) with respect to the inertia parameter was found to be not as important as the variation of ($Gr_l$) and ($Gr_u$) with respect to Prandtl number. Therefore, the detecting of the importance of inertia effect on qualitative changes in flow behaviour may not be practical. It was mentioned that across the extent of ($Gr_l < Gr < Gr_u$), two variant superposed flow structures namely; two-cell and four-cell secondary flows, might be generated relying on the kind of perturbation enforced as well as on the initial condition. Moreover, there is no critical Prandtl number above or below which dual solutions cases to exist, and such parametric dependence indicates a fold catastrophe.

Moreover, mixed convection from a permeable isothermal vertical plate filled with a non-Newtonian power-law fluid-saturated porous medium in the presence of surface injection or suction at a uniform velocity was tested by Ibrahim et al. [92]. They used nonlinear governing boundary-layer equations, which are solved numerically with implicit finite difference technique. The analysis was performed for the buoyancy assisting forced flow condition; therefore, it was assumed that ($T_w > T_\infty$) for upward flow and ($T_\infty > T_w$) for downward flow. It was deduced that, in addition to the non-Darcy parameter, the augmenting of surface mass transfer parameter enlarges the momentum and thermal boundary layers thickness, and then causes a reduction in heat transfer rates. It was also seen that increasing values of the viscosity index leads to decline the Nusselt number for both the two cases of suction and injection.

Conversely, Rami et al. [93] studied laminar mixed convection in a porous layer saturated with a Newtonian fluid confined by a vertical impermeable flat plate at constant temperature and concentration on the basis of boundary layer approximations. The results appeared that the inertial parameter ($K^2 u_D v$) tends to decrease the velocity and creates more uniform flow field due to the form drag of the porous layer. The results also showed that increasing the inertial parameter thickens the thermal and concentration boundary layers, and then increase the temperature and concentration. However, it was apparent that lower heat and mass transfer rates occur as this parameter raises.

Barletta and Rees [94] did analytical analysis for buoyancy-induced instability of mixed convective flow in a horizontal porous channel taking into account the quadratic form-drag contribution in the model of momentum transport using the Darcy–Forchheimer formulation. The top and bottom surfaces are assumed to be supplied to a symmetric constant surface cooling or heating. Longitudinal, transverse, global oblique rolls for low-amplitude perturbations were studied. They found that the commencement of the convective instability for the circumstances of boundary cooling and boundary heating is completely symmetrical. It was also found that the longitudinal rolls are the major unstable mode stimulating the instability at the lowermost Darcy–Rayleigh numbers. They investigated the neutral condition of the flow stability for several values of Péclet number and the form-drag parameter.

### 2.2.2. Darcy–Brinkmann mixed convection

The impact of a solid boundary on fluid flow in porous media supplies momentum diffusion owing to viscous resistance for high-porosity close to solid walls. Therefore, this effect is anticipated to be significant in a medium with high-porosity or more particularly when heat transfer is existed, because the convection process is typically a boundary phenomenon. It cannot be ignored although the existence of porous solid matrix in the flow field, and was added as a viscous term ($\mu' \nabla^2 u$) to the Darcy model by Brinkmann [8] to develop Darcy–Brinkmann model as follows:

$$\frac{dp}{dx} = -\frac{\mu_f}{K u_D} + \mu' \nabla^2 u, \tag{3}$$

where ($\mu'$) is the effective viscosity. This additional viscous term, which represents the frictional drag forces between the fluid layers themselves, is also called the "Brinkmann term" and satisfies the no-slip boundary condition on the impermeable solid boundaries.

Once again, Islam and Nandakumar [68] used Brinkman–Darcy model to investigate the mixed convection flow of a Newtonian fluid in a horizontal porous duct for the bottom heated and uniform temperature around periphery case. Similar to their study Islam and Nandakumar [91], the bifurcation phenomenon and dual solutions were also observed, but the multiplicity was checked for channel aspect ratio ($AR = 0.3 - 3.0$) and Grashof number ($Gr = 10 - 11500$). Their results

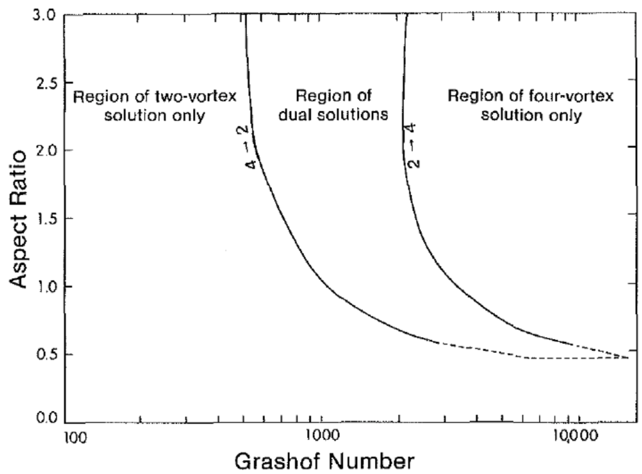


**Fig. 17.** The cusp catastrophe curves reported by Islam and Nandakumar [68] for dual solutions as a function of Gr and $AR$.

explained that the non-linearity of convective term in the momentum equation does not appear to cause of this phenomenon, where it is expected to be produced from the manner in which the momentum and energy equations are coupled. Also, the use of the Brinkman model for accounting the no-slip state did not change the qualitative behaviour considerably in the region of low permeability. Furthermore, it was observed that the variation of the critical Grashof number, at which the changeover from one mode of behaviour (the two-cell or four-cell pattern) to the another, with aspect ratio could be interpreted in terms of a cusp catastrophe shown in Fig. 17. Thus, by increasing Grashof number gradually, the intensity of the secondary flows raises with a progressive reconstruction of the two-vortex solution in the vicinity of the hot lower surface of the channel. After reaching a critical value of Grashof number called an upper critical Grashof number, the double-cells become unsteady and leads abruptly to a stable four-cell solution. Then, this flow structure is persistent with more increasing in Grashof number. However, commencing from a four-cells flow pattern, as Grashof number decreases, and after reaching a lower critical Grashof number, the flow alters suddenly into a twin-cell flow pattern. Therefore, Fig. 17 shows that there is a range of Grashof number, depending of the channel aspect ratio, where the two solutions are possible, presenting a hysteresis conduct. Similar phenomenon was observed experimentally by Buretla and Berman [67] and numerically by Chao and Hwang [66] using Darcy's law.

Al-Hadhrami et al. [95] did an analytical analysis using perturbation techniques, and a numerical solution using Brinkmann equation, to examine the influence of viscous dissipation on the thermal and flow characteristics within two vertical walls composed of a porous substrate. The temperature of the outer wall decreases linearly with the duct height ($T_w = T_{wo} - \Lambda(xH_c)$), where ($T_{wo}$) is the wall temperature at the origin level, and ($\Lambda$) is a uniform temperature gradient applied vertically along the walls. The flow was analysed in the regions of the critical Rayleigh numbers when both the viscous dissipation and Darcy effect are present. It was demonstrated that there are multi-valued solutions at, or near to the first critical Rayleigh number due to the non-linear term in the energy equation. In addition, the influence of the Darcy number declines with increasing the critical Rayleigh number in the absence of the viscous dissipation. Whereas, when the viscous dissipation is included, the velocity and buoyancy distributions seem to be independent of this parameter with decreasing Darcy number, and hence these solutions are to be equivalent to solving the linearised system.

Wong and Saeid [96] employed the same physical configuration, e.g. a jet impingement cooling of a heater immersed in a horizontal confined porous channel, studied previously by Saeid and Mohamad [71] for an isothermal heater, and later by Sivasamy et al. [72] for a fixed heat flux, using Darcy's law. Wong and Saeid [96] extended their works by employing Brinkman–Darcy model to examine the steady-state of thermal and flow characteristics in both non-Darcy and Darcy regimes. Also, the buoyancy effects were assumed to be generated from an isothermal heater with a length assuming to be twice the porous layer thickness. The average heat transfer was found to decrease with an increase of Darcy number for the non-Darcy regime (Da $\leq 10^{-4}$) when the Péclet number is low (Pe $< 30$). However, when Péclet number is high, the average heat transfer is enhanced with an increase of Darcy number for the same regime. Sivasamy et al. [97] studied similar physical problem of Wong and Saeid [96] using the same Brinkman–Darcy model, but this time for unsteady condition. The study was conducted for many parameters; Reynolds number ($1 \leq \mathrm{Re} \leq 1000$), Darcy number ($10^{-6} \leq \mathrm{Da} \leq 10^{-2}$), Grashof number ($10 \leq \mathrm{Gr} \leq 100$), and porous thickness ($0.1 \leq H_p \leq 1.0$), jet opening ($0.2 \leq d \leq 2.0$). They reported that for the non-Darcy regime when Reynolds number is high, the increase in the jet width, Darcy number and/or Grashof number enhance Nusselt number; while, increasing the porous layer was found to decrease Nusselt number. Interestingly, in both studies of Wong and Saeid [96] and Sivasamy et al. [97], the results showed that for such physical problem, the mixed convection regime might produce minimal values of Nusselt number owing to the conflict between the buoyant flows and the jet flow. This conduct is demonstrated in Fig. 18 for the two studies of Wong and Saeid [96] and Sivasamy et al. [97].

Umavathi et al. [98] examined mixed convection inside a double-passage porous vertical canal split by a conductive baffle, under a consistent surface temperature of an asymmetric cooling/heating. The highly-coupled nonlinear Brinkman–Darcy was handled first analytically using the perturbation technique and then solved numerically using the finite-difference method. They focused on the impact of the mixed convection parameter, the porous parameter, viscosity ratio, Brinkman number, and the baffle position on the flow and temperature distributions as well as the heat transfer. It was discovered that the Nusselt number increases by increasing the porous parameter for both cooling or heating actions. However, the trends of Nusselt number with Brinkman number were seen to be approximately linear even in the existence of porous substrate.

Vajravelu and Prasad [99] carried out a numerical study to test mixed convective flows in a parallel-plate vertical channel filled with an anisotropic porous material using the Keller–Box finite difference method. They considered the Darcy viscous dissipation together with the Newtonian fluid dissipation into the energy transport equation. Also, they took into account the effect of temperature on the fluid properties such as viscosity, density, and thermal conductivity, and their impacts on the thermal and flow characteristics, in addition to the influences of the orientation angle of the principal axis and the anisotropic permeability ratio. It was shown that the directional anisotropic permeability ratio and the variable thermo-physical properties have the powerful trace on the system.

Basant et al. [100] and Basant et al. [101] obtained analytical solutions for a steady-periodic system of mixed convection in inclined and vertical infinitely wide channels, respectively, packed with a porous substrate. One of the channel plates is maintained at an isothermal fixed temperature, whereas the another one is warmed sinusoidally. The energy and momentum equations are first split into periodic and steady terms and then analytically solved using the undetermined coefficients method. In the first study, they analysed the influence of the oscillating frequency of heating, Prandtl number, and Darcy number on the hydrodynamic and thermal behaviours. The results showed that there is a resonance frequency can be obtained to optimise the fluctuating amplitude of the pressure drop at the channel boundaries with the temperature oscillation for each Prandtl number. It was shown that this resonance frequency increases with any increase in Prandtl number. In the second study, they considered the existence of an interior heat

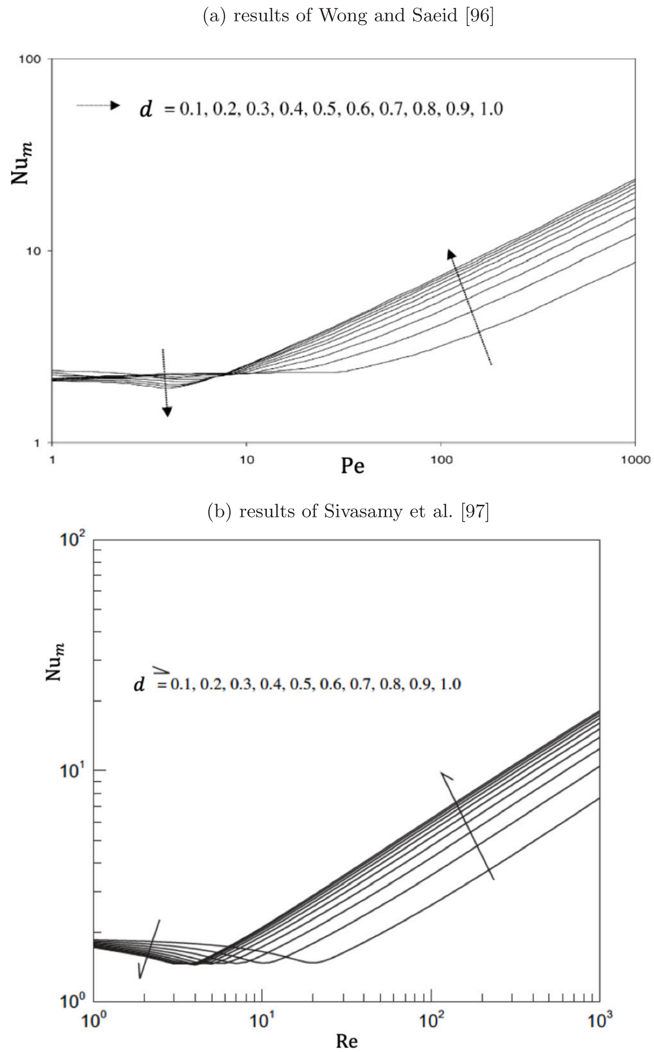


**Fig. 18.** (a) Distributions of mean Nusselt number against Pe at Ra=50 and Da=$10^{-6}$, for different jet width ($d$), presented by Wong and Saeid [96], (b) distributions of mean Nusselt number against Re at Gr=50 and Da=$10^{-4}$, for different jet width ($d$), presented by Sivasamy et al. [97]. Replotted.

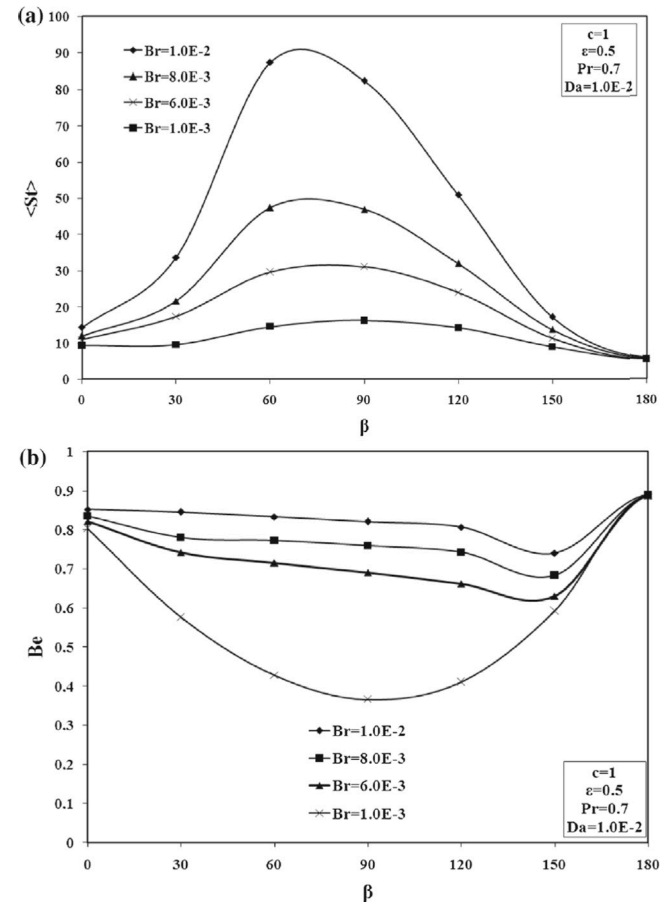


**Fig. 19.** Results of Tayari et al. [102] for the distributions of (a) the entropy generation (<St>) and (b) Bejan number, with the inclination angle ($\beta$), for various Br, and at Ra=$10^4$, Da=$10^{-2}$ and Re=10.

absorption/generation in the fluid to explore its effect as well. The results exhibited that the heat generation accelerates the convective flow, and then enhances the heat transfer rates, whereas the heat absorption does the antithesis.

Tayari et al. [102] employed an entropy generation analysis to study mixed convective flow under the viscous dissipation influence during an inclined parallel-plane plate channel stuffed with a porous substrate. A particular emphasis was provided to examine the impact of the channel inclination angle ($\beta$), varying between 0° and 180°, on the irreversibility represented by Bejan number (Be) for both transient and steady conditions. They reported that the maximum absolute entropy generation can be obtained at an inclination angle around 70°, whereas the lowest absolute entropy generation is occurred near to 0° or 180°, see Fig. 19a. In addition, it was found that the viscous fluid irreversibility becomes the dominant about 90°, for Brinkman number (Br $\leq 10^{-3}$), while for Brinkman number (Br $> 10^{-3}$), the dominance turns to the heat transfer irreversibility for all angles of inclination, see Fig. 19b.

Tayari et al. [103] did similar analysis of Tayari et al. [102] but for mixed convective flow within a Poiseuille–Benard porous channel to investigate the influence of many parameters such as Rayleigh, Darcy, and Brinkman numbers as well as the porosity on the irreversibility owing to viscous dissipation and heat transfer. The results revealed that at constant Brinkman number (Br = $10^{-3}$), Rayleigh number (Ra = $10^4$), and Darcy number (Da = 1.0), the overall entropy generation fluctuates periodically for porosity ($\varepsilon \geq 0.2$), which depicts the commencement of thermo-convective swirls during the channel. Moreover, it was shown that the entropy generation decreases when the Darcy number increases from $10^{-6}$ to $10^{-4}$ due to the domination of the viscous irreversibility. Whereas, the influence of Rayleigh number becomes significant for (Da $> 10^{-2}$), which describes the beginning of the convection effects to be prominent.

Avramenko et al. [104] performed an analytical modelling and numerical simulations, employing the lattice Boltzmann method, to study mixed forced and natural convection throughout vertical flat and circular micro-channels filled with a porous medium exposed to slipping boundary conditions. They investigated the effects of Rayleigh and Knudsen (slippage) numbers and the medium porosity on thermal and hydrodynamic profiles, the rates of heat transfer, and the friction factor. The results demonstrated that when Rayleigh number is low, the reduction in Darcy number produces a considerable increase in the hydraulic resistance and an enhancement in the energy transport. Though, when Rayleigh number increases and becomes high, these trends turn to the contrary. They compared the quantitative results of the flat channel with these of the circular channel and found that the cross-sectional form of channel can make a crucial impact on the flow behaviour and the heat transfer.

Manish et al. [105] reported the results of weakly nonlinear and linear stability analysis comprising the limited-amplitude expansion technique. They investigated the instability mechanism of mixed convective flow in a vertical channel differentially heated and packed with a quite pervious porous substrate using the Darcy–Brinkman formulation. They presented results for oil- and water-saturated porous media, with considering the participation of viscous dissipation. The results of the linear stability revealed that the flow stability declines as the Darcy number and/or Reynolds number increase. The results of the weakly nonlinear stability disclosed a supercritical bifurcation for the two fluids. Also, Shankar et al. [106] reported results for the linear stability analysis of the same problem considered by Manish et al. [105] employing the Chebyshev collocation method. They presented the curves of the neutral stability and obtained the critical wave number, Darcy–Rayleigh number, and the wave speed for various parameters such as Prandtl number and the pressure gradient.

### 2.2.3. Darcy–Brinkmann–Forchheimer mixed convection

The literature reveals that there have been several numerical and analytical works done investigating mixed convection in porous beds using the Brinkman–Forchheimer-extended Darcy model (generalised model), which includes the boundary and inertia non-Darcian effects simultaneously. Hwang and Chao [107] tested the effect of peripheral wall conduction on mixed convection in the thermally and hydrodynamically fully developed area of a horizontal square porous channel under peripherally and axially constant heat fluxes, with a finite wall thermal conductivity and thickness. The wall heat conduction parameter ($K_P$) was introduced within the thermal boundary conditions to indicate to the significance of wall heat conduction on the convection inside the channel. The flow and heat transfer characteristics were found to be extremely influenced by the non-uniform peripheral temperature variations during the wall. This is owing to the combined effects of non-infinite wall conduction parameter, non-axisymmetric channel configuration, and the buoyancy-induced secondary flows. In addition, it was found that the strength of secondary flows at the wall heat conduction of ($K_P = 10^4$) is much stronger than that at ($K_P = 0.1$).

In vertical porous channels, Hadim [108] and Hadim and Chen [109] studied mixed convective flows within porous media confined by double impermeable vertical plates, for both non-Darcy and Darcy regimes using the generalised momentum equation. The effects of asymmetric heating boundary condition and Darcy number on the flow and heat transfer for both uniform wall temperature (UWT) and uniform wall heat flux (UHF) conditions were examined numerically by Hadim [108]. The case when buoyancy impacts are assisting the upward flow was assumed, with particular emphasis on the developing region. It was obvious that for constant Reynolds and Grashof numbers, an augmentation in mixed convection heat transfer can be achieved by decreasing Darcy number. Also the heat transfer enhancement is robust and more noticeable in the (UWT) condition. Hadim and Chen [109] investigated the same case of Hadim [108], but for channel comprising discrete heat sources. They also found that as Darcy number decreases, the rates of heat transfer increase. It was shown that the influence of this parameter becomes significant around the first heater and in the non-Darcian regime.

Similar to the analytical analyses performed by Aldoss et al. [54,55] and Aldoss et al. [56] for analysing Darcian mixed convection in horizontal porous channels, Aldoss et al. [110] analysed a non-Darcian mixed convective flow inside a columnar cylinder immersed in a porous substrate. Also, similar to the work of Aldoss et al. [110], the governing equations were formulated to cover the entire regime of mixed convection with one non-similar variable within the range of ($\chi = 0 - 1$), where ($\chi = 0$) for pure natural convection (NCDR) and ($\chi = 1$) for pure forced convection (FCDR). They investigated the effect of two sorts of wall heating conditions namely; Variable wall temperature (VWT) with the power law form ($T_w - T_\infty = ax^n$) and variable heat flux (VHF) with the power law form ($q_w = bx^m$), on the heat transport rates. For such physical case, the ranges of the exponents ($m$) and ($n$) were considered as follows: ($-0.5 \le m \le 1$) and ($0 \le n \le 1$). The results indicated that higher values of heat transfer rates were associated with bigger ($n$) and ($m$), as demonstrated in Fig. 20. It was mentioned that the reason for this heat transfer augmentation is that the thickness of thermal boundary layer becomes smaller at high values of ($n$) and ($m$), consequently the thermal gradient on the wall becomes higher. It was also shown that by increasing the effect of inertia forces produces a noticeable decrease in the local Nusselt number during the mode of (NCDR), and an increase in it during the mode of (FCDR), for both (VWT) and (VHF) cases.

Chen et al. [111] tested both buoyancy-assisted and buoyancy-opposed forced flows within a perpendicular porous channel with a symmetrical uniform heat flux imposed at the boundaries. The wall temperatures were assumed to increase linearly with the wall height ($T_w = T_o + ay$), where ($a$) is a constant and ($T_o$) is the reference temperature. For the buoyancy-aided flow, the buoyancy forces work to accelerate the fluid speed in the area near the wall; therefore, it was found that Nusselt number augments when Rayleigh number is increased. They also reported that the rate of this increase is higher when Darcy number is large, similar to Avramenko et al. [104], and/or Forchheimer number is small, which was priorly proven by Rami et al. [93]. However, for the buoyancy-opposed flow, the buoyancy force acts to diminish the velocity field and decline the Nusselt number with increasing Rayleigh number and/or Darcy number. This finding was drawn by Lai et al. [78] for opposing flows inside a vertical porous channel using Darcy's law under particular circumstances.

Umavathi et al. [112] examined the problem of mixed convective flows during a vertical porous channel, analytically by the perturbation series method with absence of inertia term, and numerically by finite-difference method with South-Over-Relaxation technique in the presence of inertia forces. They deemed three different surface thermal circumstances namely; isothermal–isothermal, isoflux–isothermal, and isothermal–isoflux. Forchheimer drag term was found to have a substantial effect on the flow conduct particularly for unequal surface temperature, where it decreases the flow speed and causes recirculating flows close to the solid boundaries. Also, the effect of flow reversal was seen to be enhanced by the viscous dissipation in the case of downward while it is opposed in the case of upward inside the channel.

Kumar et al. [113] considered four variant models namely; Darcy–Brinkman (DB), Darcy–Brinkman–Wooding (DBW), Darcy–Brinkman–Forchheimer (DBF), Darcy–Brinkman–Forchheimer–Wooding (DBFW), to study buoyant-aided mixed convection in a perpendicular channel loaded with a porous material. They performed a linear stability analysis to investigate the effect of various terms emerging in the momentum formulation on the flow stability. The results showed that the effects of the inertia term, the fluid viscosity term, and the permeability term of the porous medium on the stabilising and destabilising the flow depends strongly on Prandtl number, Reynolds number, and Darcy number. In addition, in the majority of cases considered, it was found that the perturbation in the flow demeanour for the DBF model is identical to that for the DB model, and for the DBFW model is similar to that for the DBW model. In an endeavour to comprehend the kinetics of combined forced flow, due to an external pressure gradient, and buoyancy-induced free convective flow inside a standing porous pipe, Kumar et al. [114] performed analytical and numerical study to examine its reliance on some parameters of the porous medium used. They adopted non-Darcy Brinkman–Forchheimer–Wooding momentum model with assuming that the temperature of pipe surface changes linearly with vertical coordinate. The results indicated that for the buoyancy-aided flow case, reversed flow was observed at the centre of the pipe at larger Rayleigh numbers. However, For the buoyancy-counter flow case, the back flow was shown at the proximity of the pipe boundary. This can be seen in Fig. 21 for the influence of Rayleigh number on the longitudinal velocity profiles ($W_o$) across the pipe radius ($r$).

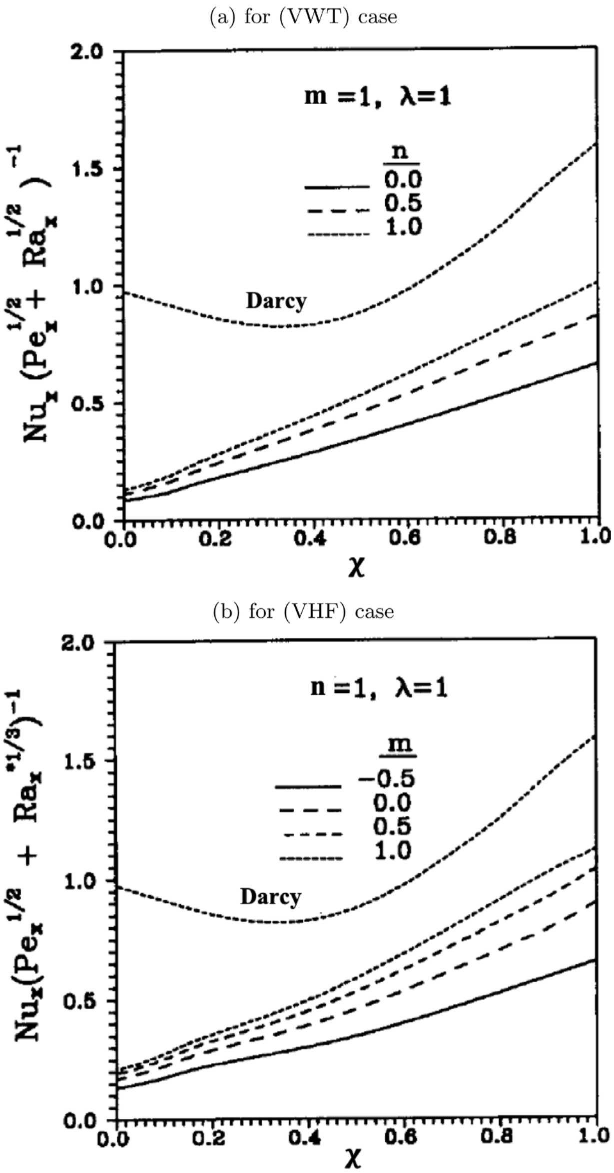


**Fig. 20.** Variations of local Nusselt number ($Nu_x$) with singular non-similarity parameter ($\chi$) for (a) (VWT) case at chosen ($n$) values, and (b) (VHF) case at chosen ($m$) values, along a columnar cylinder with curvature parameter ($\lambda$=1), reported by Aldoss et al. [110]. (Replotted)..

Umavathi and Veershetty [115] reported analytical and numerical solutions for mixed convective flows within a vertical porous channel subjected to boundary conditions of third kind, employing Brinkman–Forchheimer–Darcy model. Each of two different and equal reference temperatures for the incoming fluid, together with both different and equal Biot numbers were deemed. They investigated the impacts of different parameter such as inertia term, porous parameter, and perturbation parameter on the flow comportment, temperature dispensation, and heat transfer rates. The results displayed that for the opposing flow, the flow velocity decreases and the temperature increases with increasing the Brinkman number, while for the assisting flow, both the flow temperature and velocity fields and temperature increase with increasing the Brinkman number. It was also displayed that the inertia and porous parameters restrain the fluid flow, for the two different boundary conditions considered above for Biot number and reference inlet temperature.

Adeniyan and Abioye [116] conducted an analytical analysis to inspect the momentum and heat transfer in a columnar duct with its left wall connected to a definite thickness of Darcy–Forchheimer porous substrate, whereas its right wall is exposed to a uniform temperature. They considered the effects of viscous dissipation, Rose-land radiation, and permeability. They studied the impacts of Reynolds, Grashof, Darcy, Brinkman, Stark (or conduction–radiation parameter), and Forchheimer numbers, as well as the thermal conductivity ratio. It was shown that the rates of heat transfer and skin-friction coefficient increase as Grashof and Brinkman in addition to the conductivity ratio increase for small values of Forchheimer numbers. However, the heat transfer and friction coefficient were found to decrease with the width of the porous substrate for large values of Forchheimer numbers. It was also found that increasing Stark number by magnifying the radiation parameter can increase Nusselt numbers.

Sharma and Bera [117] conducted linear stability analysis of combined natural and forced convective parallel flows in a vertical highly penetrated porous canal employing the Darcy–Brinkman–Forchheimer model. The canal is assumed to be isothermally and differentially warmed along its entire left and right walls. The investigation was conducted for several Prandtl numbers including air, water, mercury, and heavy oils, and for a broad range of Reynolds number. The results illustrated that each type of fluid generates different flow instability. For instance, the mercury causes a thermal-shear instability, the heavy oils as well as the water trigger the thermal-buoyant instability, while the air produces the interactive instability. Different to Sharma and Bera [117], Sharma et al. [118] published results of finite amplitude nonlinear stability analysis of mixed convective flow in a vertical porous channel having surface temperatures linearly vary with the vertical axis, using the Brinkman–Forchheimer–Darcy equation. They provided results for air- and water-saturated porous media, with taking into account the involvement of viscous dissipation. The aim of their investigation is to analyse the bifurcation nature and the conduct of unsteady disruptions of limited amplitude. This can happen behind the linear instability limitation, particularly whenever the flow intensity and the porous medium permeability are fairly large. Their results demonstrated that once using water as a working fluid, the unique sort of bifurcation obtained at and behind the bifurcation level is the supercritical bifurcation. Though, when using a porous medium saturated by air, two kinds of bifurcations namely; subcritical and supercritical, were noticed, relying on the permeability and flow strength.

In horizontal porous channels, Wong and Saeid [119] extended the works of Saeid and Mohamad [71], Sivasamy et al. [72], Wong and Saeid [96], and Sivasamy et al. [97] for the problem of a cooling jet impinging vertically a heater submerged in a porous substrate confined by double horizontal plates. Saeid and Mohamad [71] and Sivasamy et al. [72] used Darcy's law, whereas Wong and Saeid [96] and Sivasamy et al. [97] employed Brinkman–Darcy model. On the other hand, Wong and Saeid [119] used the steady-state Brinkman–Forchheimer-extended Darcy model to tested the effect of inertial coefficient of a porous medium ($C_F$) and its porosity ($\varepsilon$) on the average Nusselt number. The results showed that the mixed convection mode is emerged in the moderately high values of Péclet number (Pe) at which minimum Nusselt number is found. For the Darcy regime ($Da \le 10^{-4}$), the porosity and the inertial coefficient showed trivial impacts on Nusselt number, where the variation of Nusselt number is diminished when ($C_F \ge 0.2$), and this variation is negligible for the range of porosity ($0.7 \le \varepsilon \le 0.95$), see Fig. 22. However, for the non-Darcy regime, the effects of these parameters are only significant in the forced convection domination region when ($Pe > 200$), in which the increase in any one of them reduces Nusselt number.

The same authors Wong and Saeid [120] investigated numerically unsteady mixed convective flows arising from a low speed air jet impinging vertically a block of metal foam heat sink inside a horizontal channel. The porous medium was selected to have a fixed high porosity of 0.97 to enabling the mixed oscillatory flow to develop throughout the medium. Also, they fixed the values of effective/fluid thermal conductivity ratio of 1.2 and the inertia coefficient of 0.1. While, the

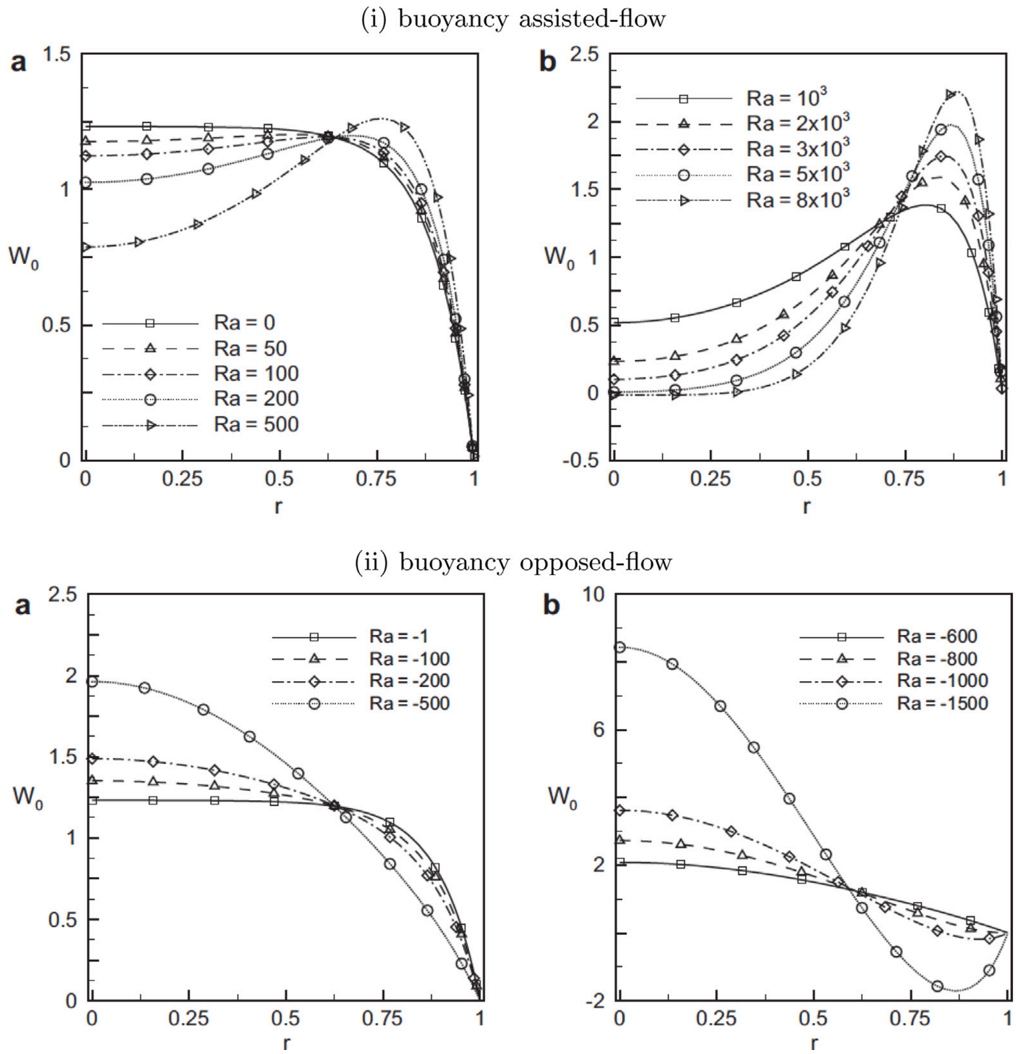


**Fig. 21.** Results of Kumar et al. [114] showing the influence of Ra on the longitudinal velocity profiles ($W_o$) across the pipe radius ($r$), for (i) buoyancy assisted-flow and (ii) buoyancy opposed-flow.

impacts of Darcy number between ($1 \times 10^{-5} \leq \mathrm{Da} \leq 5 \times 10^{-4}$), Rayleigh number between ($2 \times 10^5 \leq \mathrm{Ra} \leq 1 \times 10^6$), and Péclet number between ($10 \leq \mathrm{Pe} \leq 1000$) on the flow conduct within the channel and heat transfer rate. Their results revealed that no numerical convergence or steady-state solution can be obtained when the thermal system is in the regime of mixed convection, i.e. ($\mathrm{Ra} \geq 4 \times 10^5$) and ($200 \leq \mathrm{Pe} \leq 1000$), as shown in Fig. 23. Instead, the results showed a periodic behaviour for the average Nusselt number, displayed in Fig. 24, caused by the oscillation convection owing to the conflict for domination between the forced convective jet flow and the buoyancy-induced convective flow. This behaviour was also reported by Saeid and Pop [70] and Saeid and Mohamad [71] for a physical system entirely filled with a porous medium. However, the oscillation convections in the current study are more difficult as they occur in two different physical regions namely, porous heat sink and clear fluid without a porous medium. They also investigated the effects of the heat sink height and the effective/fluid heat capacity ratio on the oscillatory convection. Thus, it was found that the amplitude and frequency of the oscillatory periods increase with increasing the heat capacity ratio, indicating to that porous substances with large heat capacity are a desirable environment for oscillatory convections. It was also found that increasing the height of the porous heat sink increases the oscillatory period amplitude, but decreases its frequency.

In another study about jet-impingement cooling a porous heat sink, Saeid et al. [121] investigated steady mixed convective flow of a vertical air jet cooling a metal-fibrous heat sink located inside a horizontal channel. They examined the influence of six various shapes of heat sink on the flow and thermal behaviours throughout the channel, and on the average heat dissipation from the heat sink. Two types of aluminium foam namely; G10 and G20, were used, and they are different only in their permeabilities, i.e. $2.843 \times 10^{-7}$ and $1.229 \times 10^{-7}$ ($m^2$), respectively. The shapes considered were rectangle, triangle, opposite triangle, trapezoidal, opposite trapezoidal, and elliptic. Their numerical study covered broad ranges of Reynolds number ($\mathrm{Re} = 100 - 400$) and Grashof number ($\mathrm{Gr} = 0, 5712, 19278, 45696$), e.g. representing cases of with ($\mathrm{Gr} > 0$) and without ($\mathrm{Gr} = 0$) the buoyancy effect, as well as with and without the presence of fibrous heat sink for a good qualitative comparison. First of all, they did not report oscillatory convective flows in the channel as Wong and Saeid [120] reported, due to considering the steady-state governing equations.

Their results showed that the rate of heat dissipation might be enhanced by more than 95% when covering the heat source by a metal foam comparing with the case of without metal foam. In addition, it was shown that utilising aluminium foam type G10 is much better than type G20 for good heat transfer argumentation due to its higher permeability. Interestingly, it was found that the influence of heat sink shape on the heat dissipation relies vigorously on the mode of heat transfer and Reynolds number. Thus, in the force convection when ($\mathrm{Gr} = 0$) and for high Reynolds number ($\mathrm{Re} > 300$), the convex shapes

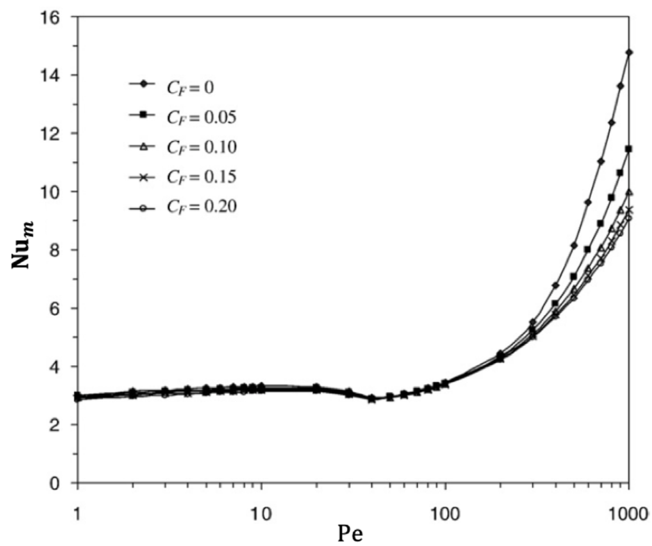


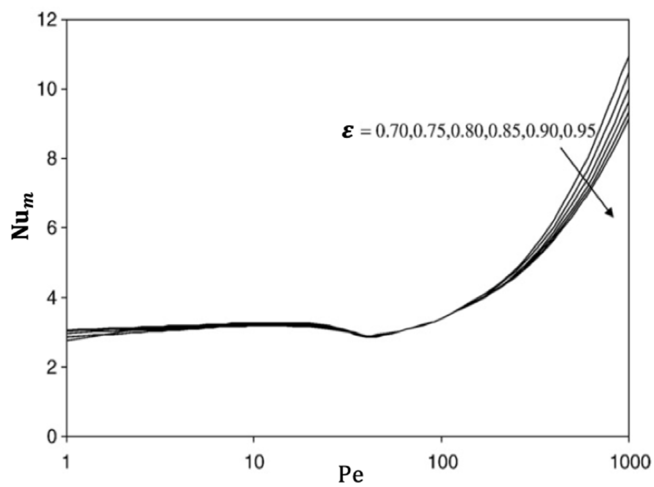


**Fig. 22.** Variation of average Nusselt number ($Nu_m$) versus Pe for (Top) various inertial coefficient ($C_F$), and (Bottom) various porosity ($\varepsilon$), presented by Wong and Saeid [119]. (Replotted).

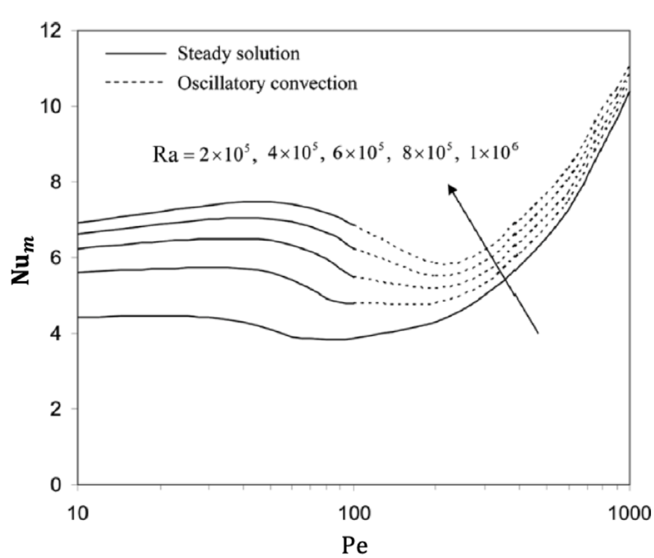


**Fig. 23.** Variation of Nusselt number versus Pe for various Ra at Da=5×10$^{-4}$, presented by Wong and Saeid [120]. (Replotted).

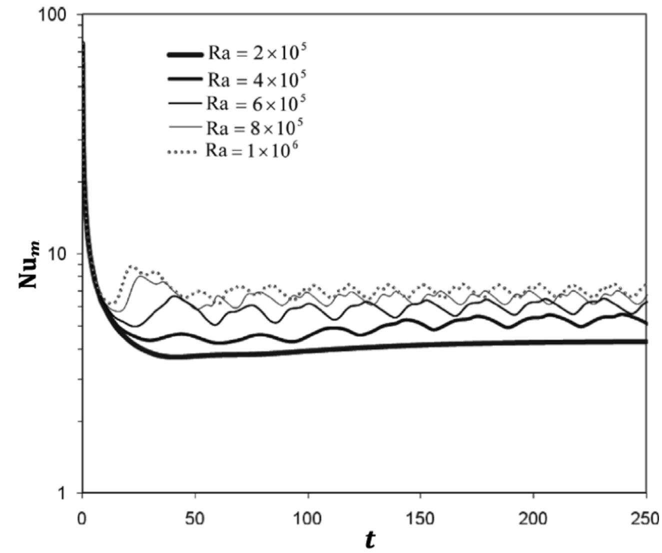


**Fig. 24.** Variation of the average Nusselt number with time showing the oscillation convection for various Ra at Da=5×10$^{-4}$ and Pe=200, reported by Wong and Saeid [120]. (Replotted).

were found to be more effective for heat transfer. However, for Grashof number (Gr > 0) and low Reynolds number (Re < 200), the results indicated that the concave shapes are preferably for better heat transfer augmentation.

Combined forced and free convective flows in horizontal fluid superposed porous layers subjected to a finite heat source from the bottom surface, illustrated in Fig. 25, is investigated numerically and experimentally by Dixon and Kulacki [122,123], respectively. They studied the effects of Rayleigh number, Péclet number, Darcy number, conductivity ratio, as well as the height of porous bed on the flow behaviour and rates of heat transfer. The results of both studies identified the presence of a critical values of Péclet number and porous layer thickness at which Nusselt number has lowest values.

Buonomo et al. [124] conducted both numerical and experimental analyses for mixed convection of air-flow within a horizontal conduit partly packed with an aluminium foam under the heating action by a constant heat flux from below. The investigations were carried out for different sorts of foam, i.e. 10, 20, 40 PPI, and for Richardson number varying between (1 ≤ Ri ≤ 2000), and Reynolds number varying between (5 ≤ Re ≤ 250). Results of temperature and velocity distributions were obtained for the two cases of with and without porous medium. It was found that the flow configuration in the empty channel is parabolic, e.g. having the peak value at the centre of the channel, whereas it becomes more uniform within the metal foam, particularly for small flow speeds. The results also affirmed that the utilisation of metal foam inside the channel, increasing Reynolds number, and/or increasing Richardson number, augment considerably the rates of heat transfer, as shown in Fig. 26 as an example for their experimental results.

Mohammed et al. [125] investigated computationally similar physical problem investigated numerically by Lai et al. [58], Lai et al. [59], Prasad et al. [60], Lai and Kulacki [63], Lai et al. [62], Lai and Kulacki [64], Saeid and Pop [70] and Ozgen and Varol [76], and experimentally by Lai and Kulacki [65], for mixed convection inside a horizontal porous channel heated from the bottom by a localised heater, for different thermal boundary conditions. The thermal boundary conditions considered by Mohammed et al. [125] are as follows; the lower horizontal surface is assumed to be insulated excepting the heater, whereas the upper surface is considered to have the same inlet flow temperature. Lai et al. [58], Lai et al. [59], Prasad et al. [60], and Ozgen and Varol [76] solved the steady-state form of simple Darcy

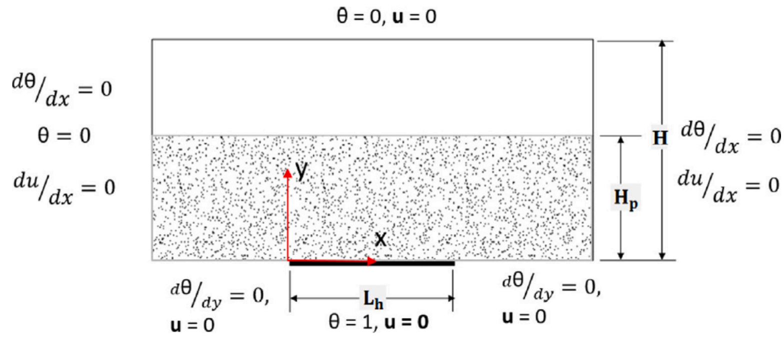


**Fig. 25.** Physical configuration studied numerically by Dixon and Kulacki [122] and experimentally by Dixon and Kulacki [123].

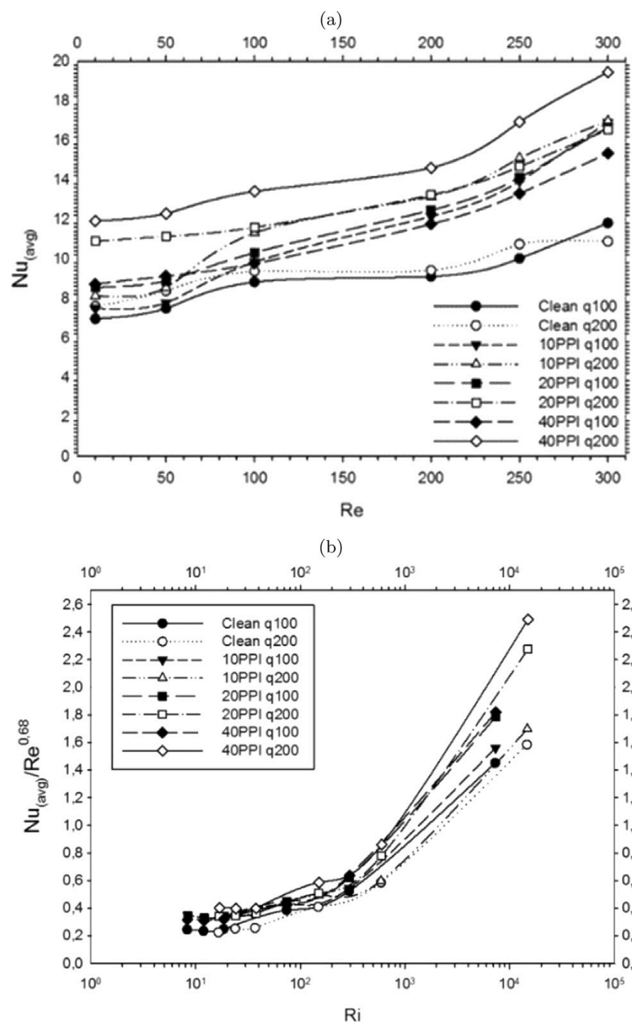


**Fig. 26.** Results of Buonomo et al. [124] showing (a) the variation of average Nusselt number with Re, and (b) the ratio of ($Nu_{(avg)}$/Re) with Ri, for different sorts of foams 10, 20 and 40 PPI.

model; however, Lai and Kulacki [63], Lai et al. [62], Lai and Kulacki [64], and Saeid and Pop [70] solved the unsteady form of Darcy model. Therefore, Mohammed et al. [125] extended their works by solving the problem employing the transient Darcy–Brinkman–Forchheimer model for momentum. They investigated the influences of Reynolds number ($Re = 0.1 - 50$) and Richardson number ($Ri = 1 - 100$) in both porous and clear channels, as well as the impacts of porosity ($\varepsilon = 0.7 - 0.95$) and Darcy number ($Da = 0.1 - 100$) for the porous channel. It was deduced that the existence of porous material enhances the values

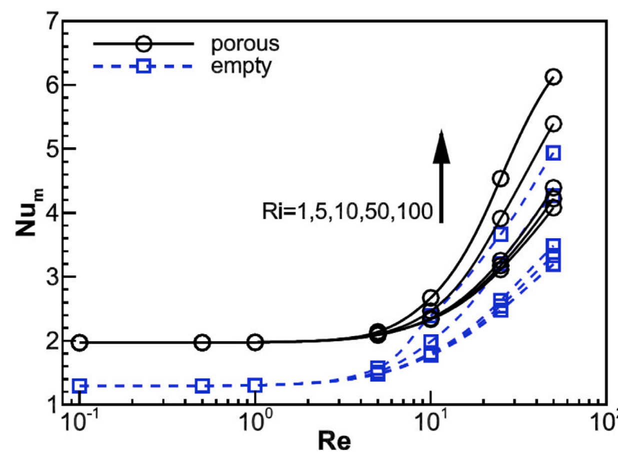


**Fig. 27.** Results of Mohammed et al. [125] showing the variations of mean Nusselt number in porous and empty channels for various Ri and Re.

of Nusselt number; however, it does not change the tendency of the variations of Nusselt number, as illustrated in Fig. 27. In addition, it was predicted that oscillatory unstable convective flows are produced in both porous and clear channels for higher Reynolds and Richardson numbers. The amplitude and period of oscillations were observed to be different in the two channels, and the flow instability in the clear channel is greater than that in the porous channel. For comparison, they presented the flow and thermal behaviours in both channels as well as the time-evaluation of the mean Nusselt numbers. Fig. 28 displays part of their results for the oscillatory flow behaviours in the two channels at ($Re = 50$) and ($Ri = 100$). It is worth mentioning that such convection oscillations were observed previously by Lai et al. [62], Lai and Kulacki [63], Lai and Kulacki [64], Lai and Kulacki [65] and Saeid and Pop [70], but as mentioned before for different boundary conditions.

It is worth noting that all aforementioned works have not considered the thermal dispersion effect and the channelling effect in their studies.

### 2.3. Considering thermal dispersion and channelling effect

A phenomenon that occurs in all flows through porous media, and which need to be considered into account is the "thermal dispersion". The impact of the inter-particle conduction or the thermal dispersion on energy transport process is an important topic in this media. The mixing of local fluid streams in the presence of a temperature difference across the porous medium yields an enhancement in the transport energy, which is generally represented by a diffusive heat flux. Cheng and Vortmeyer [22] investigated the impact of transverse thermal dispersion on forced convection in the fully-developed region

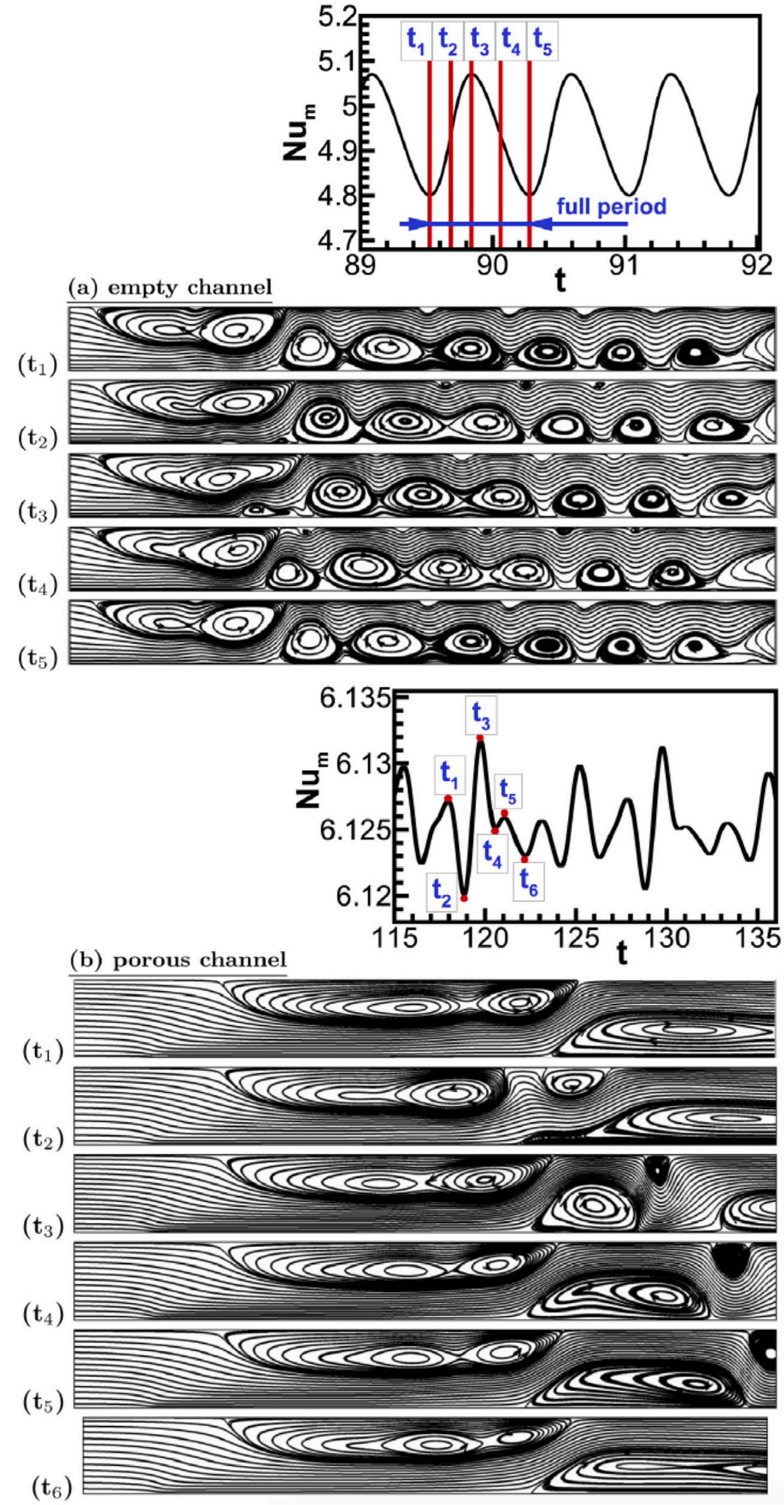


**Fig. 28.** Oscillatory flow behaviours over one period in (a) empty channel, and (b) porous channel, at Re=50 and Ri=100, reported by Mohammed et al. [125].

of a packed bed bounded between parallel plates. Moreover, constant-porosity assumption is inappropriate for some applications, such as fixed bed catalytic reactors, packed bed heat exchangers, and drying and metal processing. It has been recognised that the confining impermeable boundary of the packed bed influences its porosity. That is, the porosity is high close to a wall and declines to an asymptotic value in the core of porous domain. Therefore, the region in the vicinity of external impermeable boundary is of particular importance, since heat transfer and fluid flow and other mechanisms are closely involved in that region and all sensitive to variations in porosity. Vafai [126] analysed experimentally and theoretically the channelling effect on the forced convection flow along an isothermal flat plate, and found that the channelling effect has a significant influence on the heat transfer augmentation for high porosity and high Reynolds number conditions. Cheng and Hsu [127] tested the effect of solid wall on the thermal dispersion in forced convection flows during an annular packed bed of spheres. Generally speaking, the inclusion of thermal dispersion and flow maldistribution effects aid in augmenting the energy transport process and their incorporation in the simulation would, thus, provide better simulation of the actual problem.

Chen et al. [128] and Chen [129] included the near-wall porosity variation and thermal dispersion effects in their mathematical models to study mixed convection in a porous layer. They considered the porous layer to be close to a vertical or horizontal plates and with variable temperature and heat flux, respectively. Their mathematical models were solved using the Boussinesq and boundary-layer approximations. Single non-similarity mixed convection parameter was inserted for covering the whole mixed convection zone. It was found that the non-Darcian effects alter the flow and thermal characteristics from those simulated using the Darcy equation. Also, the influences of no-slip boundary condition and the flow inertia were found to have tending to decrease the flow speed and energy transport. However, the variable porosity effect was shown to improve the momentum and thermal transports through the boundary layer due to the channelling effect. Consequently, this produces a great enhancement in heat transfer because of the dispersive transport phenomenon that causes a good convective mixing throughout the pores. The local Nusselt number can be either increased or decreased when these effects along with fluid inertia and boundary friction are considered depending on the interaction amongst different influences of non-Darcy flow phenomena and heating conditions at the wall.

A steady mixed convective non-Darcian flow in a three-dimensional horizontal channel packed with spheres has been the subject for researches done by Chou and Chung [130] and Chang et al. [131] for the same thermal heating conditions. Chou and Chung [130] examined the influence of stagnant conductivity, which is involved inside the effective thermal conductivity in the energy equation, on convective flow and thermal characteristics inside a square channel, displayed in Fig. 29. The channel was assumed to be under two thermal boundary conditions namely; constant axial heat flux and constant circumferential wall temperature. The stagnant conductivity was characterised based on the solid-to-fluid thermal conductivity ratio ($K_r = k_s k_f$). Water-stainless steel spheres bed ($K_r = 26.8$, Pr = 6.5), air-glass spheres ($K_r = 38.8$, Pr = 0.71), water-glass spheres ($K_r = 1.3$, Pr = 6.5), and the case of ($K_r = 100$), were investigated to clarify the impact of stagnant conductivity. Both Nusselt numbers and the hydrodynamic pattern of buoyancy-induced secondary flows were found to be magnificently affected by the stagnant conductivity for low values of Péclet number, where the thermal dispersion impact is weak. It was predicted that (126%) of heat transfer enhancement is obtained when Rayleigh number increases from (0) to ($10^5$) at certain value of ($K_r = 1.3$), but only (21%) and (7.9%) are estimated in the cases of ($K_r = 26.8$) and ($K_r = 100$) respectively. Whereas, Chang et al. [131] disregarded the nonlinear inertia term in the non-Darcian momentum equation, and assumed the flow in fully hydro-dynamically developed and thermally developing regions at the entrance of the heated section. It was deduced that secondary flow induced by buoyancy effect becomes stronger and heat transfer is higher with increasing Rayleigh number and decreasing Péclet number. However, the thermal dispersion effect induced by Péclet number which is also very important dominates the buoyancy effect when it increases.

Interestingly, it is worth declaring here that all non-Darcian effects including the fluid inertia, boundary viscous resistance, thermal dispersion, and variable porosity have been merely taken into account in the studies mentioned in this section for the mode of mixed convection in porous channels under local thermal equilibrium ($LTE$) condition, that is, using one-equation energy model.

### 2.4. Considering local thermal non-equilibrium model

In porous media, the phase temperatures can be differing on the basis of the thermo-physical properties of each phase as well as the nature of the transient process. Indeed, in many thermal applications like regenerators, nuclear rods located in an intercooler coolant pathway,

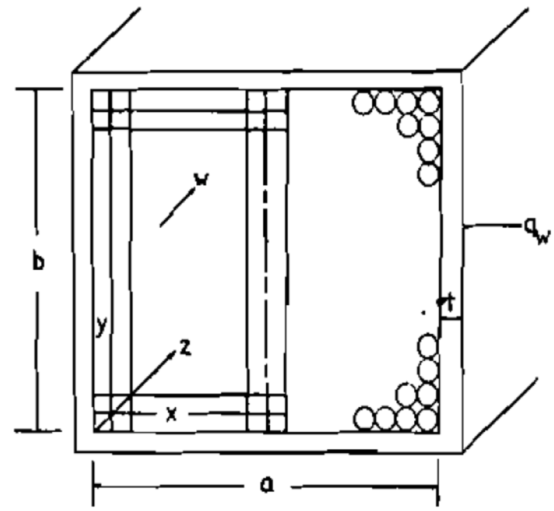


**Fig. 29.** The physical problem solved by Chou and Chung [130].

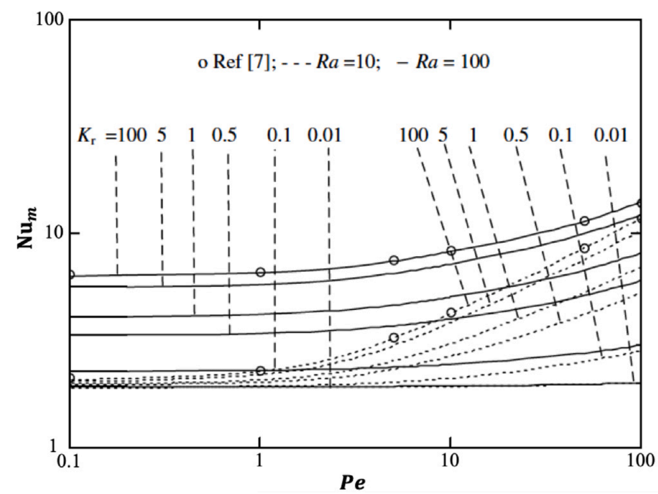


**Fig. 30.** This figure was reported Saeid [132] for the comparison between their results of total average Nusselt number using ($LTNE$) model and the results published by Lai et al. [78] using ($LTE$) model, showing that the huge difference between them at low $K_r$. (Replotted).

thermal energy storages in buried repositories, the temperature discrepancy between the fluid phase and the solid phase is vital. Therefore, two energy approximations, which is called local thermal non-equilibrium ($LTNE$) model, are substantially required for calculating thermal field for each individual phase.

Saeid [132] carried out a numerical investigation of mixed convective assisting and opposing flows in a vertical porous layer adjacent to a vertical plate employing the thermally non-equilibrium energy ($LTNE$) model. They studied the impacts of the interfacial convective heat transfer parameter ($H_v$) and the ratio of thermal conductivity ($K_r$) on heat and flow characteristics. The mixed convection is prompted by a segment isothermally heated and placed on the vertical plate in the existence of externally-pressured aiding or opposing flow. Similar physical problem was considered by Lai et al. [78] who investigated opposing and aiding mixed convective flows in a vertical porous plate channel employing the thermally equilibrium energy ($LTE$) model. Saeid [132] conducted a comparison between the two models to verify the validity of the ($LTNE$) model for ($0.01 \le H_v \le 100$) and ($0.01 \le K_r \le 100$). The results revealed that for low values of $H_v$ and $K_r$, the thermal equilibrium ($LTE$) model might not be able to estimate the mean Nusselt number correctly in both opposing and aiding flows. Fig. 30 reported by Saeid [132] shows

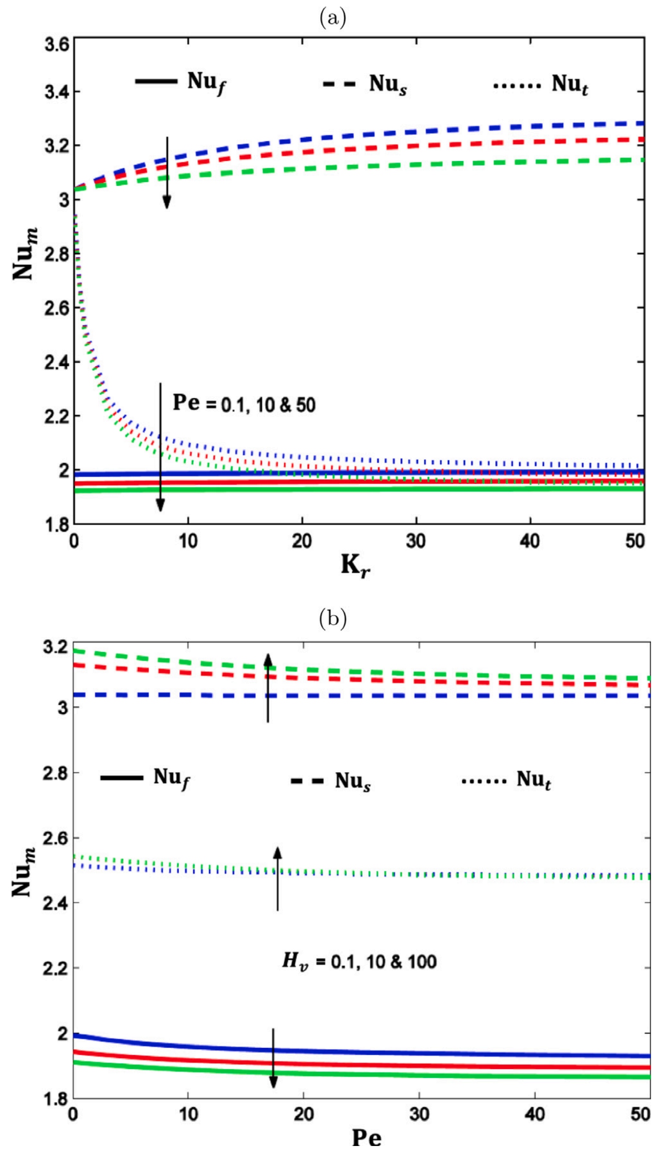


**Fig. 31.** The impacts of (a) thermal conductivity ratio ($K_r$) and (b) interfacial heat transfer parameter ($H_v$), on $\mathrm{Nu}_f$, $\mathrm{Nu}_s$, and $\mathrm{Nu}_t$, for different Pe, reported Ahmed et al. [133]. Replotted).

the huge difference in the total average Nusselt number between the two aforementioned models ($LTE$) and ($LTNE$) at lower thermal conductivity ratio. However, for higher values of these parameters $H_v$ and $K_r$, the thermal equilibrium model can calculate correctly the mean Nusselt number as well as the temperature field.

Saeid [134] extended the work done by Saeid and Mohamad [71] who tested the interaction between a horizontal cross-flow and a vertical jet in a horizontal porous layer under the thermal equilibrium assumption, to consider the thermal non-equilibrium circumstance. It is worth noting that this case was also studied later by Wong and Saeid [96], Wong and Saeid [119], Sivasamy et al. [72], Sivasamy et al. [97], under the thermal equilibrium condition, but for different momentum models. Saeid [134] assumed the heat source length ($L_h$), which is located on the bottom surface, to be two times the thickness of porous layer ($H_p$), with assuming the jet width ($d$) as ($dH_p = 0.1$). It was found that the higher mean Nusselt numbers were predicted using the local thermal equilibrium ($LTE$) model, and the heat transfer rates are substantially declined in the existence of a wake flow with a vertical jet. Also, it was found that higher Nusselt numbers might be reproduced for

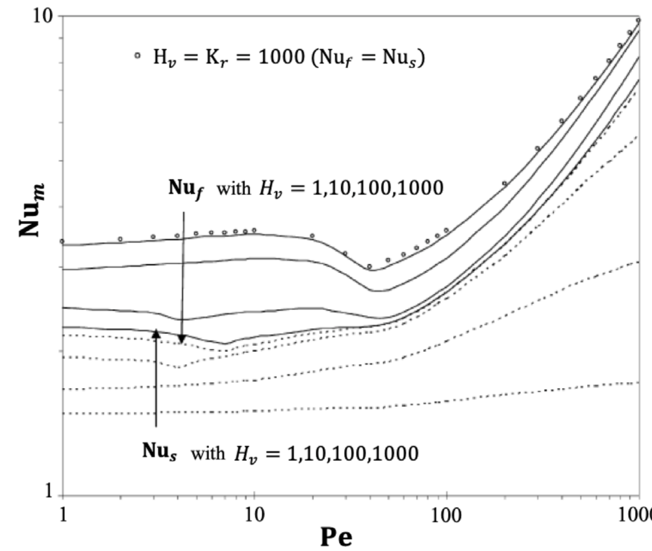


**Fig. 32.** This figure was presented Wong and Saeid [135] for the impact of $H_v$ on $\mathrm{Nu}_f$ and $\mathrm{Nu}_s$ for different Pe, and at $K_r = 1$, $\varepsilon = 0.78$, Da= $10^{-3}$, Ra= 100. (Replotted).

higher values of the interfacial heat transfer coefficient and the thermal conductivity ratio.

Rees [136] studied the influence of the local thermal non-equilibrium on the stability of mixed convection in a vertical porous channel uniformly cooled and heated from the boundaries, using a linear energy stability analysis. It was found that the thermal system remains always stable to low-amplitude disturbances of all wave numbers, and for all Darcy–Rayleigh numbers. Ahmed et al. [133] used the ($LTNE$) model to study mixed convection and radiation inside an annular perpendicular cylinder stuffed with a porous substrate, for assisting and opposing flows. They investigated the impacts of Péclet number (Pe), porosity-scaled fluid/solid thermal conductivity ratio ($K_r$), and interfacial convective heat transfer parameter ($H_v$) on the heat transfer during the solid ($\mathrm{Nu}_s$) and fluid ($\mathrm{Nu}_f$) phases, at Rayleigh number of (Ra = 100) and radiation parameter of ($R_d = 0.5$). Importantly, it was reported that the discrepancy between $\mathrm{Nu}_f$ and $\mathrm{Nu}_s$ increases as ($K_r$) or ($H_v$) increases, in both aiding and opposing flow cases, referring to the prevalence of the thermal non-equilibrium in the system. Fig. 31 demonstrates their results for the effect of ($K_r$), ($H_v$) and (Pe) in the assisting flow.

However, in the aforementioned studies of Saeid [132,134],Rees [136] and Ahmed et al. [133], the simple Darcy model was used. Wong and Saeid [135,137] investigated numerically the mixed thermal characteristics of the air jet impingement cooling of confined flat porous bed subjected to the condition of local thermal non-equilibrium, employing the Brinkman–Forchheimer–Darcy model. Wong and Saeid [135] conducted their study for many parameters including; Rayleigh number (Ra = 10 – 200), Péclet number (Pe = 1 – $10^4$), Darcy number (Da = $10^{-6} - 10^{-3}$), porosity-scaled thermal conductivity ratio ($K_r = 1 - 10^3$), porosity ($\varepsilon = 0.75 - 0.99$), and interfacial heat transfer coefficient parameter ($H_v = 1 - 10^3$). Their focus was to demonstrate the Darcian and non-Darcian effects in the mixed convection regime. They also found that the ($LTNE$) becomes invalid for low values of $H_v$ and $K_r$, where the values of average fluid Nusselt number ($\mathrm{Nu}_f$) diverge from these of average solid Nusselt number ($\mathrm{Nu}_s$), as shown in Fig. 32. Also, it was illustrated that the increase in the porosity increases the total average heat transfer rate, however its influence becomes smaller when the value of the thermal conductivity ratio is small.

Whereas, Wong and Saeid [137] studied opposing mixed convective flows raised from an air-jet cooling of a hot horizontal wall by impinging it inside an open cavity, which is installed inside a horizontal canal stuffed with high porosity (FeCrAlY) metal foam. The thermal

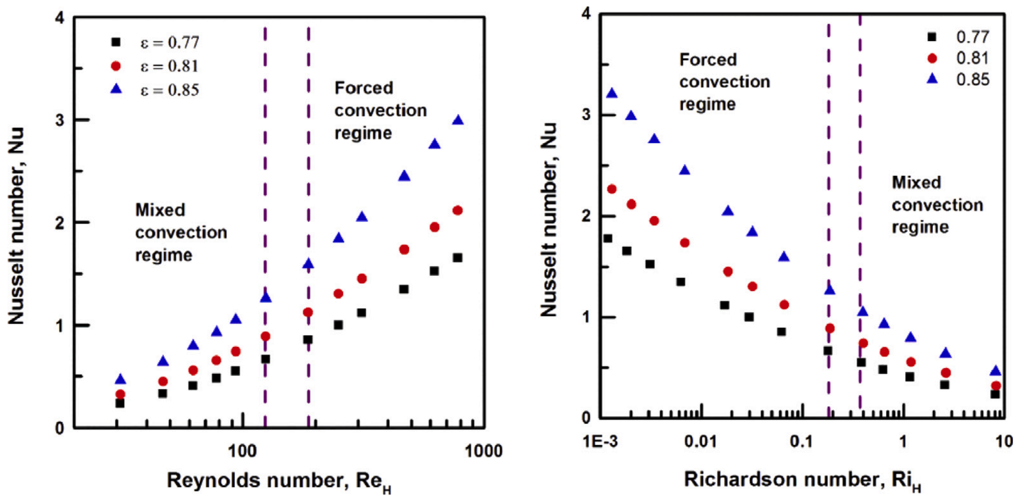


**Fig. 33.** Results of Kotresha and Gnanasekaran [138] for the variation of Nu with (Left) Re, and (Right) Ri, for different $\varepsilon$.

characteristics for different cavity height ($0 \leq H_c \leq 0.4$) and Rayleigh number ($Ra = 50 - 150$) were tested and compared to the case without cavity. Their results disclosed that the cavity absence case produces the highest values of fluid and solid mean Nusselt numbers $Nu_f$ and $Nu_s$, respectively, and these values decrease with the enlargement in the cavity height. Minimum $Nu_f$ is acquired at the range of Péclet number ($Pe = 30 - 60$) which depends on the value of Rayleigh number and the cavity depth, and it becomes more noteworthy at greater Rayleigh numbers as a result of the contra mixed convective flows. However, it was also found that $Nu_s$, is unaffected by the variation of Rayleigh number and the cavity depth for a wide range of ($Pe = 1 - 10^3$). In fact, this attitude of a lowest mean Nusselt number for the case of the cavity presence is the same to that stated by Wong and Saeid [96,135] for the case without cavity, in which opposing influences between the upward buoyancy forces and the vertical jet flow gives inferior rates of heat transfer.

Khandelwal and Bera [139] extended the work of Chen et al. [111] trying to figure out the effect of the thermal non-equilibrium condition on mixed convective opposing and aiding flows inside a perpendicular parallel porous channel adopting the non-Darcy–Brinkman–Forchheimer equation. Similar to Chen et al. [111], the channel is assumed to be under a symmetrical uniform heat flux imposed at the walls; thus, the wall temperatures increase linearly with the height. The highly coupled governing equations, ($LTNE$) and ($DBF$), were solved computationally using the spectral Collocation technique and analytically when the drag term ($F$) and the thermal conductivity ratio ($\gamma$) are assumed equal to zero. They investigated the impacts of different parameters such as Forchheimer number, Darcy number, Rayleigh number, thermal conductivity ratio, and inter-phase heat transfer coefficient on the hydrodynamic conduct of fluid flow the heat transfer, for each buoyancy opposed and assisted situations. Generally, it was found that an increase in the inter-phase convective coefficient fabricates a soft and stabilised fluid flow in the porous channel, and retrieves the mechanism similar to the equilibrium case. However, raising the medium conductivity ratio was found to destabilise considerably the fluid flow by creating a flow disconnection and an inflection point on the profiles of velocity. Moreover, similar to Chen et al. [111] in the thermal equilibrium state, they also reported that the increase in Darcy number leads to a reduction in the rates of heat transfer at low thermal conductivity ratio ($\gamma$), but for the whole range of the inter-phase convective coefficient.

Buonomo et al. [140] studied numerically transient mixed convection heat transfer in a parallel-plate vertical channel stuffed an aluminium foam of constant porosity of ($\varepsilon = 0.909$), and halfway heated at regular heat flux. The half lower parts of the channel walls were heated the other two half upper parts were deemed to be insulated. The investigation was conducted employing the local thermal non-equilibrium state between the two phases, and the Brinkman–Forchheimer-extended Darcy formulation, for various geometrical aspect ratios (the heated part) and Reynolds number. They found that Nusselt number decreases as the geometrical aspect ratio increases or Reynolds number decreases. The results showed that the aspect ratio has a significant influence on the energy transport within the solid phase more than within the fluid phase, and the effect of Reynolds number was more pronounced within the fluid phase.

Numerical simulations of buoyancy-supported mixed convective flows a perpendicular canal packed with a highly permeated brass wire mesh were performed by Kotresha and Gnanasekaran [138] using the Darcy–Forchheimer equation under the effect of the local thermal non-equilibrium condition. The brass mesh is joined to an aluminium slab, which is placed inside the vertical canal as a heat source, thereby the consequent system develops to be conjugate heat transfer. It was reported that the augmentation in heat transfer by inserting the brass wire mesh is doubled more than that without the porous medium. Also, increasing the mesh porosity causes a reduction in the pressure drop, but generates a further enhancement in heat transfer. Thus, it was found that increasing the porosity of the wire mesh from 0.77 to 0.81, increases Nusselt number (Nu) 1.41 times, and from 0.77 to 0.85 increases (Nu) 1.86 times, see Fig. 33. Kotresha et al. [141] studied the same physical problem of Kotresha and Gnanasekaran [138] using the same momentum and energy models. They investigated the effect of using four kinds of aluminium foam with PPI 10, 20, 30, and 45 that covering the porosity from 0.90 to 0.95, on the velocity and temperature profiles and the heat transfer, for variant Reynolds and Richardson numbers. Their results revealed that the value of Nusselt number increases as the PPI of the metal foam enlarges; however, this advantage was occurred on the expense of pressure drop. It was found that the metal foam with 30 PPI is the best option for higher thermal performance comparing with other foams.

Leela et al. [142] presented results for mixed convection heat transport inside a vertical microporous parallel plate channel with internal heat generation and viscous dissipation and internal heat generation employing the Brinkman–Darcy momentum equation under the assumption of local thermal non-equilibrium ($LTNE$). The effect of considering the ($LTNE$) condition on the buoyancy-aided convective flows was investigated for variable surface heat flux and variable surface temperature boundary conditions. Also, they discussed the impacts of some main parameters like Rayleigh, Brinkman, and Darcy numbers, as well as the porosity scaled thermal conductivity ratio, the inter-phase convective coefficient ($LTNE$ parameter), and the interior heat generation. The numerical results showed that the heat dissipation rates increase as Rayleigh number and/or the interior heat generation increase, for both boundary conditions considered. It was also shown that the improvement in the $(LTNE)$ parameter reduces the heat transfer, and Darcy number does not have any influence on the variation of Nusselt number.

## 3. Conclusions

In the above literature, the majority of the studies that have investigated mixed convection problem in porous channels used the early simple Darcy's formulation to represent the fluid motion. However, other studies that have taken the non-Darcian effects into consideration neglected the important other effects such as the porosity variation through the domain which affects the flow field significantly particularly in the vicinity of the solid boundary, and the thermal dispersion, which influences the heat transfer characteristics in both the longitudinal and the transverse directions. It has been claimed that the later effect cannot be ignored once the non-Darcy effects become prevalent. Regarding to the energy transport, it is expected that when there is a significant difference between advection and conduction mechanisms in transferring heat, which in involved in many applications, the divergence between fluid and solid phases temperatures enlarges, and then the thermal equilibrium condition becomes invalid. The current literature reveals that a quite interest has been exerted in the area of mixed convective heat transfer in a fluid-saturated porous media utilising the two-equation energy model.

In summary, the studies that have been achieved so far for initiating an appropriate model for mixed convection inside channels filled with a porous material, comprising some streamlining presumptions for instance adoption of $(LTE)$ condition, disregarding of the porosity variation, or omitting the effect of thermal dispersion, have been first reported. Then, the works of non-Darcain laminar mixed convection, in which the influences of boundary, inertia, channelling effect, and the inclusion of thermal dispersion under thermal non-equilibrium $(LTNE)$ condition are incorporated, have been recorded.

### Nomenclature

| | |
|---|---|
| $a, b$ | constants. |
| $A$ | ratio of heater length to height of porous layer $(A = L_h/H_p)$. |
| $AR$ | duct aspect ratio, (width height). |
| Be | Bejan number. |
| Bi | Biot number. |
| Br | Brinkman number. |
| $C_F$ | inertial coefficient. |
| $d$ | jet width, (m). |
| $d_p$ | particle diameter, (m). |
| Da | Darcy number, Da=$K/H^2$. |
| $F$ | geometry function (Forchheimer term). |
| $g$ | gravitational acceleration, (m/s$^2$). |
| Gr | Grashof number, $Gr = g.\beta.\rho^2.H^3.(T_h - T_o)/\mu^2$. |
| $\mathrm{Gr}_l$ | lower critical Grashof number. |
| $\mathrm{Gr}_u$ | upper critical Grashof number. |
| $H_c$ | channel or cavity height, (m). |
| $H_p$ | height of porous layer, (m). |
| $H_w$ | solid wall thickness, (m). |
| $H_v$ | interfacial convective heat transfer parameter. |
| $k_f$ | fluid thermal conductivity, (W/m K). |
| $k_s$ | solid thermal conductivity, (W/m K). |
| $K$ | permeability, (m$^2$). |
| $K_r$ | thermal conductivity ratio, $(k_s/k_f)$. |
| $K_p$ | wall heat conduction parameter. |
| $L_h$ | length of heater, (m). |
| $L_c$ | channel length, (m). |
| $L_d$ | distance between two heaters, (m). |
| $m, n$ | constants. |
| $\mathrm{Nu}_m$ | mean Nusselt number. |
| $p$ | dimensional pressure, (N/m$^2$). |
| Pe | Péclet number, Pe=Re.Pr. |
| $\mathrm{Pe}_x$ | local Péclet number, Pe=Re$_x$.Pr. |
| Pr | Prandtl number. |
| $q$ | heat flux, (W/m$^2$). |
| $r$ | pipe radius, (m). |
| Ra | Rayleigh number, Ra= $g.\beta_f.H^3.(T_w - T_o)/\alpha_f.\nu_f$. |
| $\mathrm{Ra}_x$ | local Rayleigh number, Ra= $g.\beta_f.x^3.(T_w - T_o)/\alpha_f.\nu_f$. |
| $\mathrm{Ra}_{crit}$ | critical Rayleigh number |
| Re | Reynolds number, Re=$u_o.\rho_f.H/\mu$. |
| Ri | Richardson number, Ri=Gr/Re$^2$. |
| $T_c$ | cold temperature, $(°C)$. |
| $T_h$ | hot temperature, $(°C)$. |
| $T_o$ | reference temperature, $(°C)$. |
| $T_w$ | wall temperature, $(°C)$. |
| $T_{wo}$ | wall temperature at the origin level, $(°C)$. |
| $T_\infty$ | free-stream temperature, $(°C)$. |
| <St> | average total entropy generation, (J s$^{-1}$ K$^{-1}$). |
| $u_\infty$ | free-stream horizontal velocity, (m/s). |
| $u_D$ | Darcian velocity, (m/s). |
| $\mathrm{W}_o$ | non-dimensional longitudinal velocity. |
| $x, y$ | dimensional Coordinates, (m). |

#### Greek symbols

| | |
|---|---|
| $\alpha_r$ | thermal diffusivity ratio, $(\alpha_s/\alpha_f)$. |
| $\beta$ | coefficient of volumetric expansion, $(°C^{-1})$. |
| $\boldsymbol{\beta}$ | channel inclination angle, (°). |
| $\lambda$ | curvature parameter of columnar cylinder. |
| $\Lambda$ | uniform temperature gradient applied along the wall. |
| $\rho_f$ | density, (kg/m$^3$). |
| $\varepsilon$ | porosity. |
| $\phi$ | non-dimensional temperature. |
| $\mu_f$ | fluid dynamic viscosity, (N s/m$^2$). |
| $\mu'$ | effective dynamic viscosity, (N s/m$^2$). |
| $\nu_f$ | fluid kinematic viscosity, (m$^2/s$). |
| $\zeta$ | inertia parameter. |
| $\xi_{(forced)}$ | non-similarity parameter covering forced convection region. |
| $\xi_{(natural)}$ | non-similarity parameter covering natural convection region. |
| $\chi$ | single non-similarity parameter. |
| $\chi'_{(x)}$ | local single non-similarity parameter for variable wall temperature (VWT) condition. |
| $\chi^*_{(x)}$ | local single non-similarity parameter for variable heat flux (VHF) condition. |
| $\Gamma$ | dimensionless pressure gradient (flow parameter). |

#### Subscripts

| | |
|---|---|
| $c$ | cold. |
| $h$ | hot. |
| $o$ | reference point. |
| $f$ | fluid. |
| $s$ | solid. |
| $w$ | wall. |
| $\infty$ | free-stream. |

### Declaration of competing interest

The authors declare that they have no known competing financial interests or personal relationships that could have appeared to influence the work reported in this paper.

## Acknowledgement

This research was supported in part by the Monash eResearch Centre and eSolutions-Research Support Services through the use of the MonARCH HPC Cluster.

## Funding

This research did not receive any specific grant from funding agencies in the public, commercial, or not-for-profit sectors.

## References

[1] M. Kaviany, Principles of Heat Transfer in Porous Media, second ed., Springer-Verlag, New York, 1995.
[2] R.G. Carbonell, S. Whitaker, Heat and mass transfer in porous media, in: J. Bear, M.Y. Corapcioglu (Eds.), Fundamentals of Transport Phenomena in Porous Media, Martinus Nijhoff, Dordrecht (Boston), 1998, pp. 121–198.
[3] M. Quintard, S. Whitaker, One- and two-equation models for transient diffusion processes in two-phase systems, Adv. Heat Transf. 23 (1993) 369–464.
[4] K. Vafai, A. Amiri, Non-darcian effects in confined forced convective flows, in: D.B. Ingham, I. Pop (Eds.), Transport Phenomena in Porous Media, Pergamon, An Imprint of Elsevier Science, 1998, pp. 313–329.
[5] D.A. Nield, A. Bejan, Convection in Porous Media, third ed., Springer Science+Business Media, New York, NY, USA., 2006.
[6] H. Darcy, Les Fontaines Publiques De La Ville De Dijon, Victor Dalmont, Paris, 1856.
[7] P.H. Forchheimer, Wasserbewegung durch boden, Zeitschrift Vereines Deutscher Ingenieure 45 (50) (1901) 1782–1788.
[8] H.C. Brinkmann, A calculation of the viscous force exerted by a flowing fluid on a dense swarm of particles, Appl. Sci. Res. 1 (1) (1949) 27–34.
[9] R.A. Wooding, Steady state free thermal convection of liquid in a saturated permeable medium, J. Fluid Mech. 2 (1957) 273–285.
[10] T.E.W. Schumann, Heat transfer: A liquid flowing through a porous prism, J. Franklin Inst. B 208 (3) (1929) 405–416.
[11] B.W. Gamson, G. Thodos, O.A. Hougen, Heat, mass and momentum transfer in the flow of gases through granular solids, Trans. AIChE 39 (1943) 1–35.
[12] A.G. Dixon, D.L. Cresswell, Theoretical prediction of effective heat transfer parameters in packed beds., AIChE J. 25 (4) (1979) 663–676.
[13] N. Wakao, S. Kaguei, T. Funazkri, Effect of fluid dispersion coefficients on particle-to-fluid heat transfer coefficients in packed beds- correlation of nusselt numbers, Chem. Eng. Sci. 34 (3) (1979) 325–336.
[14] E. Achenbach, Heat and flow characteristics of packed beds, Exp. Therm. Fluid Sci. 10 (1) (1995) 17–27.
[15] F. Kuwahara, M. Shirota, A. Nakayama, A numerical study of interfacial convective heat transfer coefficient in two-energy equation model for convection in porous media, Int. J. Heat Mass Transfer 44 (6) (2001) 1153–1159.
[16] M. Moghari, A numerical study of non-equilibrium convective heat transfer in porous media, J. Enhanc. Heat Transf. 15 (1) (2008) 81–99.
[17] S. Yagi, D. Kunii, Studies on effective thermal conductivities in packed beds, Chem. Eng. Prog. 3 (3) (1957) 373–381.
[18] S. Yagi, N. Wakao, Heat and mass transfer from wall to fluid in packed beds, AIChE J. 5 (1) (1959) 79–85.
[19] S. Yagi, D. Kunii, N. Wakao, Studies on axial effective thermal conductivities in packed beds, AIChE J. 6 (4) (1960) 543–546.
[20] P. Cheng, Thermal dispersion effects in non-Darcian convective flows in a saturated porous medium, Lett. Heat Mass Transf. 8 (4) (1981) 267–270.
[21] J. Levec, R.G. Carbonell, Longitudinal and lateral thermal dispersion in packed beds. Part II: Comparison between theory and experiment, AIChE J. 31 (4) (1985) 591–602.
[22] P. Cheng, D. Vortmeyer, Transverse thermal dispersion and wall channelling in a packed bed with forced convective flow, Chem. Eng. Sci. 43 (9) (1988) 2523–2532.
[23] S.M. Kuo, C.L. Tien, Transverse dispersion in packed-sphere beds, in: ASME Proceedings of the Heat Transfer Conference, Vol. 96, New York, NY, USA, 1988, pp. 629–634.
[24] C.T. Hsu, P. Cheng, Thermal dispersion in a porous medium, Int. J. Heat Mass Transfer 33 (8) (1990) 1587–1597.
[25] D.B. Ingham, I. Pop, Transport Phenomenon in Porous Media, Vol. 2, Oxford, Pergamon, 1998.
[26] D.A. Nield, A. Bejan, Convection in Porous Media, second ed., Springer, Berlin, 1999.
[27] H. Hadim, K. Vafai, Overview of current computational studies of heat transfer in porous media and their applications-forced convection and multiphase heat transfer, Adv. Num. Heat Transf. 2 (2000) 291–330.
[28] K. Vafai, H. Hadim, Overview of current computational studies of heat transfer in porous media and their applications-natural and mixed convection and multiphase heat transfer, Adv. Num. Heat Transf. 2 (2000) 331–371.
[29] K. Vafai, Handbook of Porous Media, Marcel dekker, New York, 2000.
[30] I. Pop, D.B. Ingham, Convective Heat Transfer: Mathematical and Computational Modelling of Viscous Fluids and Porous Media, Oxford, Pergamon, 2001.
[31] A. Bejan, A.D. Kraus, Heat Transfer Handbook, Wiley, New York, 2003.
[32] D.B. Ingham, A. Bejan, E. Mamut, Emerging Technologies and Techniques in Porous Media, Kluwer, Dordrecht, 2004.
[33] A.E. Bergles, Applications of heat transfer augmentation, in: S. Kakac, A.E. Bergles, F. Mayinge (Eds.), Heat Exchangers: Thermal–Hydraulic Fundamentals and Design, Hemisphere, New York, 1981, pp. 883–911.
[34] J.P. Gupta, Fundamentals of Heat Exchanger and Pressure Vessel Technology, Hemisphere, New York, 1986.
[35] R.L. Webb, Principles of Enhanced Heat Transfer, Hemisphere, New York, 1994.
[36] E. Palm, J.E. Weber, O. Kvernvold, On steady convection in a porous medium, J. Fluid Mech. 54 (1972) 153–161.
[37] B.C. Chandrasekhara, D. Vortmeyer, Flow model for velocity distribution in fixed porous beds under isothermal conditions, Wärme- Und Stoffübertragung 12 (2) (1979) 105–111.
[38] J. Bear, M.Y. Corapcioglu, Fundamentals of Transport Phenomena in Porous Media, Martinus Nijhott, 1982.
[39] R.A. Wooding, Rayleigh Instability of a thermal boundary layer in flow through a porous medium, J. Fluid Mech. 9 (1960) 183–192.
[40] R.A. Wooding, Convection in a saturated porous medium at large Rayleigh number or péclet number, J. Fluid Mech. 15 (4) (1963) 527–544.
[41] M. Prats, The effect of horizontal fluid flow on thermally induced convection currents in porous mediums, J. Geophys. Res. 71 (20) (1966) 4835–4838.
[42] F.M. Sutton, Onset of convection in a porous channel with net through flow, Phys. Fluids 13 (8) (1970) 1931–1934.
[43] G.M. Homsy, A.E. Sherwood, Convective instabilities in porous media with through flow, AIChE J. 22 (1) (1976) 168–174.
[44] M.A. Combarnous, P. Bia, Combined free and forced convection porous media, Soc. Pet. Eng. J. 11 (4) (1971) 399–405.
[45] P. Cheng, Combined free and forced convection flow about inclined surfaces in porous media, Int. J. Heat Mass Transfer 20 (9) (1977) 807–814.
[46] P. Cheng, Similarity solutions for mixed convection from horizontal impermeable surfaces in saturated porous media, Int. J. Heat Mass Transfer 20 (9) (1977) 893–898.
[47] P. Cheng, Convective heat transfer in porous layers by integral methods, Lett. Heat Mass Transf. 5 (5) (1978) 243–252.
[48] C.T. Hsu, P. Cheng, Onset of longitudinal vortices in mixed convective flow over an inclined surface in a porous medium, J. Heat Transfer 102 (3) (1980) 544–549.
[49] C.T. Hsu, P. Cheng, Vortex instability of mixed convective flow in a semi-infinite porous medium bounded by a horizontal surface, Int. J. Heat Mass Transfer 23 (6) (1980) 789–798.
[50] W.J. Minkowycz, P. Cheng, R.N. Hirschberg, Non-similar boundary layer analysis of mixed convection about a horizontal heated surface in a fluid-saturated porous medium, Int. Commun. Heat Mass Transf. 11 (2) (1984) 127–141.
[51] B.C. Chandrasekhara, Mixed convection in the presence of horizontal impermeable surfaces in saturated porous media with variable permeability, Wärme-Und Stoffübertragung 19 (1985) 195–201.
[52] A. Nakayama, H. Koyama, General similarity transformation for combined free and forced-convection flows within a fluid-saturated porous medium, J. Heat Transfer 109 (4) (1987) 1041–1045.
[53] A. Nakayama, I. Pop, Unified similarity transformation for free, forced and mixed convection in Darcy and non-Darcy porous media, Int. J. Heat Mass Transfer 34 (2) (1991) 357–367.
[54] T.K. Aldoss, T.S. Chen, B.F. Armaly, Nonsimilarity solutions for mixed convection from horizontal surfaces in a porous medium-variable surface heat flux, Int. J. Heat Mass Transfer 36 (2) (1993) 463–470.
[55] T.K. Aldoss, T.S. Chen, B.F. Armaly, Nonsimilarity solutions for mixed convection from horizontal surfaces in a porous medium-variable wall temperature, Int. J. Heat Mass Transfer 36 (2) (1993) 471–477.
[56] T.K. Aldoss, T.S. Chen, B.F. Armaly, Mixed convection over nonisothermal horizontal surfaces in a porous medium: The entire regime, Numer. Heat Transf.: Part A: Applications 25 (6) (1994) 685–701.
[57] M. Haajizadeh, C.L. Tien, Combined natural and forced convection in a horizontal porous channel, Int. J. Heat Mass Transfer 27 (6) (1984) 799–813.
[58] F.C. Lai, F.A. Kulacki, V. Prasad, Mixed convection in horizontal porous layers: effects of thermal boundary conditions, in: ASME Proceedings of the Heat Transfer Conference, Vol. 84, New York, NY, USA, 1987, pp. 91–96.
[59] F.C. Lai, V. Prasad, F.A. Kulacki, Effects of the size of heat source on mixed convection in horizontal porous layers heated from below, in: 2nd ASME/JSME Proceedings of Thermal Engineering Joint Conference, Vol. 2, New York, NY, USA, 1987, pp. 413–419.
[60] V. Prasad, F.C. Lai, F.A. Kulacki, Mixed convection in horizontal porous layers heated from below, J. Heat Transf. Trans. ASME 110 (2) (1988) 395–402.
[61] P.H. Oosthuizen, Mixed convective heat transfer from a heated horizontal plate in a porous medium near an impermeable surface, J. Heat Transf. Trans. ASME 110 (2) (1988) 390–394.

[62] F.C. Lai, C.Y. Choi, F.A. Kulacki, Free and mixed convection in horizontal porous layers with multiple heat sources, J. Thermophys. Heat Trans. 4 (2) (1990) 221–227.
[63] F.C. Lai, F.A. Kulacki, Transient mixed convection in horizontal porous layers locally heated from below, in: ASME Proceedings of the Heat Transfer Conference, Vol. 96, Houston, TX, USA, 1988, pp. 353–364.
[64] F.C. Lai, F.A. Kulacki, Oscillatory mixed convection in horizontal porous layers locally heated from below, Int. J. Heat Mass Transfer 34 (3) (1991) 887–890.
[65] F.C. Lai, F.A. Kulacki, Experimental study of free and mixed convection in horizontal porous layers locally heated from below, Int. J. Heat Mass Transfer 34 (2) (1991) 525–541.
[66] C.H. Chao, G.J. Hwang, Laminar mixed convection in rectangular darcy porous channels with the effect of aspect ratio, J. Chin. Soc. Mech. Eng. 12 (6) (1991) 580–589.
[67] R.J. Buretla, A.S. Berman, Convective heat transfer in a liquid saturated porous layer, ASME J. Appl. Mech. 47 (1976) 249–253.
[68] R.M. Islam, K. Nandakumar, Multiple solutions for buoyancy-induced flow in saturated porous media for large péclet numbers, J. Heat Transfer, Transactions ASME 108 (4) (1986) 866–871.
[69] C.H. Chao, G.J. Hwang, Laminar mixed convection in a horizontal rectangular Darcy porous channel, J. Chin. Soc. Mech. Eng. 13 (5) (1992) 430–437.
[70] N.H. Saeid, I. Pop, Periodic mixed convection in horizontal porous layer heated from below by isoflux heater, Arab J. Sci. Eng . 31 (2B) (2006) 153–164.
[71] N.H. Saeid, A.A. Mohamad, Jet impingement cooling of a horizontal surface in a confined porous medium: Mixed convection regime, Int. J. Heat Mass Transfer 49 (21–22) (2006) 3906–3913.
[72] A. Sivasamy, V. Selladurai, P. Rajesh Kanna, Jet impingement cooling of a constant heat flux horizontal surface in a confined porous medium: Mixed convection regime, Int. J. Heat Mass Transfer 53 (2010) 5847–5855.
[73] N.H. Saeid, Mixed convection jet impingement cooling of a rectangular solid heat source immersed in a porous layer, J. Porous Media 8 (4) (2015) 401–413.
[74] L.A. Sphaier, A. Barletta, Unstable mixed convection in a heated horizontal porous channel, Int. J. Therm. Sci. 78 (2014) 77–89.
[75] A. Barletta, M. Celli, P.V. Brandão, L.S. de B. Alves, Wavepacket instability in a rectangular porous channel uniformly heated from below, Int. J. Heat Mass Transfer 147 (2020) 118993.
[76] F. Ozgen, Y. Varol, Numerical study of mixed convection in a channel filled with a porous medium, Appl. Sci. 9 (211) (2019) 9020211.
[77] M. Parang, M. Keyhani, Boundary effects in laminar mixed convection flow through an annular porous medium, J. Heat Transfer 109 (1987) 1039–1041.
[78] F.C. Lai, V. Prasad, F.A. Kulacki, Aiding and opposing mixed convection in a vertical porous layer with a finite wall heat source, Int. J. Heat Mass Transfer 31 (5) (1988) 1049–1061.
[79] I. Pop, D.A.S. Rees, C. Egbers, Mixed convection flow in a narrow vertical duct filled with a porous medium, Int. J. Therm. Sci. 43 (5) (2004) 489–498.
[80] N.H. Saeid, I. Pop, Mixed convection from two thermal sources in a vertical porous layer, Int. J. Heat Mass Transfer 48 (19-20) (2005) 4150–4160.
[81] S. Mahmud, I. Pop, Mixed convection in a square vented enclosure filled with a porous medium, Int. J. Heat Mass Transfer 49 (13-14) (2006) 2190–2206.
[82] D. Cimpean, I. Pop, D.B. Ingham, J.H. Merkin, Fully developed mixed convection flow between inclined parallel plates filled with a porous medium, Transp. porous Med. 77 (2009) 87–102.
[83] A. Barletta, Instability of mixed convection in a vertical porous channel with uniform wall heat flux, Phys. Fluids 25 (2013) 084108.
[84] A. Barletta, M. Celli, Instability of combined forced and free flow in an inclined porous channel, Int. J. Comput. Methods 13 (2) (2016) 1640001.
[85] A. Barletta, M. Miklavčič, Instability of fully developed mixed convection with viscous dissipation in a vertical porous channel, Transp. porous Med. 117 (2017) 337–347.
[86] H. Celik, M. Mobedi, Effect of an inserted porous layer on heat and fluid flow in a vertical channel with mixed convection, Therm. Sci. 19 (3) (2015) 1005–1016.
[87] K. Vafai, C.L. Tien, Boundary and inertia effects on flow and heat transfer in porous media, Int. J. Heat Mass Transfer 24 (2) (1981) 195–203.
[88] S. Ergun, Fluid flow through packed columns, Chem. Eng. Prog. 48 (2) (1952) 89–94.
[89] F.C. Lai, F.A. Kulacki, Non-Darcy convection from horizontal impermeable surfaces in saturated porous media, Int. J. Heat Mass Transfer 30 (10) (1987) 2189–2192.
[90] Z.H. Kodah, A.M. Al-Gasem, Non-Darcy mixed convection from a vertical plate in saturated porous media-variable surface heat flux, Wärme- Und Stoffübertragung 33 (5-6) (1998) 377–382.
[91] R.M. Islam, K. Nandakumar, Mixed convection heat transfer in porous media in the non-Darcy regime, Can. J. Chem. Eng. 66 (1) (1988) 68–74.
[92] F.S. Ibrahim, S.M. Abdel-Gaid, R.S. Reddy Gorla, Non-Darcy mixed convection flow along a vertical plate embedded in a non-Newtonian fluid saturated porous medium with surface mass transfer, Int. J. Numer. Method H. 10 (4) (2000) 397–408.
[93] Y.J. Rami, A.B. Fawzi, A.A.R. Fahmi, Darcy-Forchheimer mixed convection heat and mass transfer in fluid saturated porous media, Int. J. Numer. Method H. 11 (5-6) (2001) 600.
[94] A. Barletta, D.A.S. Rees, Unstable mixed convection flow in a horizontal porous channel with uniform wall heat flux, Transp. porous Med. 129 (2019) 385–402.
[95] A.K. Al-Hadhrami, L. Elliott, D.B. Ingham, Combined free and forced convection in vertical channels of porous media, Transp. porous Med. 49 (3) (2002) 265–289.
[96] K.C. Wong, N.H. Saeid, Numerical study of mixed convection on jet impingement cooling in a horizontal porous layer-using Brinkman-extended Darcy model, Int. J. Therm. Sci. 48 (1) (2009) 96–104.
[97] A. Sivasamy, V. Selladurai, P. Rajesh Kanna, Mixed convection on jet impingement cooling of a constant heat flux horizontal porous layer, Int. J. Therm. Sci. 49 (2010) 1238–1246.
[98] J.C. Umavathi, I.C. Liu, A.J. Chamkha, Mixed convection flow in a vertical channel filled with a fluid-saturated porous medium divided by a perfectly conductive baffle, Int. J. Microscale Nanoscale Therm. Fluid Transp. Phenom. 5 (2) (2014) 127.
[99] K. Vajravelu, K.V. Prasad, Mixed convection heat transfer in an anisotropic porous medium with oblique principal axes, J. Mech. 30 (4) (2014) 327–338.
[100] K.J. Basant, D. Deborah, O.A. Abiodun, Mixed convection in an inclined channel filled with porous material having time-periodic boundary conditions: Steady-periodic regime, Transp. porous Med. 109 (2015) 495–512.
[101] K.J. Basant, D. Deborah, O.A. Abiodun, Role of heat generation/absorption on mixed convection flow in a vertical tube filled with porous material having time-periodic boundary condition: Steady-periodic regime, Transp. porous Med. 111 (2016) 681–699.
[102] A. Tayari, A. Ben Brahim, M. Magherbi, Second law analysis in mixed convection through an inclined porous channel, Int. J. Thermophys. 36 (2015) 2881–2896.
[103] A. Tayari, N. Hidouri, M. Magherbi, A. Ben Brahim, Second law analysis through a porous Poiseuille–Benard channel flow, J. Heat Transfer, ASME 138 (2016) 020801.
[104] A.A. Avramenko, Y.Y. Kovetska, I.V. Shevchuk, A.I. Tyrinov, V.I. Shevchuk, Mixed convection in vertical flat and circular porous microchannels, Transp. porous Med. 124 (2018) 919–941.
[105] K.K. Manish, K.S. Abhishek, P. Bera, Instability of mixed convection in a differentially heated channel filled with porous medium: A finite amplitude analysis, Phys. Fluids 33 (2021) 024109.
[106] B.M. Shankar, J. Kumar, I.S. Shivakumara, Numerical investigation of the stability of mixed convection in a differentially heated vertical porous slab, Appl. Math. Comput. 389 (2021) 125486.
[107] G.J. Hwang, C.H. Chao, Effects of wall conduction and Darcy number on laminar mixed convection in a horizontal square porous channel, J. Heat Transfer Trans. ASME 114 (3) (1992) 614–621.
[108] H.A. Hadim, Numerical study of non-Darcy mixed convection in a vertical porous channel, J. Thermophys. Heat Trans. 8 (2) (1994) 371–373.
[109] H.A. Hadim, G. Chen, Non-darcy mixed convection in a vertical porous channel with discrete heat sources at the walls, Int. Commun. Heat Mass Transf. 21 (3) (1994) 377–387.
[110] T.K. Aldoss, M.A. Jarrah, B.J. Al-Sháer, Mixed convection from a vertical cylinder embedded in a porous medium: non-Darcy model, Int. J. Heat Mass Transfer 39 (6) (1996) 1141–1148.
[111] Y.C. Chen, J.N. Chung, C.S. Wu, Y.F. Lue, Non-Darcy mixed convection in a vertical channel filled with a porous medium, Int. J. Heat Mass Transfer 43 (13) (2000) 2421–2429.
[112] J.C. Umavathi, J.P. Kumar, A.J. Chamkha, I. Pop, Mixed convection in a vertical porous channel, Transp. porous Med. 61 (3) (2005) 315–335.
[113] J. Kumar, P. Bera, A. Khalili, Influence of inertia and drag terms on the stability of mixed convection in a vertical porous-medium channel, Int. J. Heat Mass Transfer 53 (2010) 5261–5273.
[114] A. Kumar, P. Bera, J. Kumar, Non-Darcy mixed convection in a vertical pipe filled with porous medium, Int. J. Therm. Sci. 50 (2011) 725–735.
[115] J.C. Umavathi, S. Veershetty, Non-Darcy mixed convection in a vertical porous channel with boundary conditions of third kind, Transp. porous Med. 95 (2012) 111–131.
[116] A. Adeniyan, I.A. Abioye, Mixed convection radiating flow and heat transfer in a vertical channel partially filled with a Darcy-forchheimer porous substrate, Gen. Math. Notes 32 (2) (2016) 80–104.
[117] A.K. Sharma, P. Bera, Linear stability of mixed convection in a differentially heated vertical channel filled with high permeable porous-medium, Int. J. Therm. Sci. 134 (2018) 622–638.
[118] A.K. Sharma, M.K. Khandelwal, P. Bera, Finite amplitude analysis of non-isothermal parallel flow in a vertical channel filled with a highly permeable porous medium: A finite amplitude analysis, J. Fluid Mech. 857 (2018) 469–507.
[119] K.C. Wong, N.H. Saeid, Numerical study of non-darcian effects on jet impingement cooling in a horizontal porous layer in the mixed convection regime, Int. Commun. Heat Mass Transf. 36 (1) (2009) 45–50.
[120] K.C. Wong, N.H. Saeid, Unsteady mixed convection of a confined jet in a fluid-superposed high porosity medium, Numer. Heat Transf.: A: Applications 56 (10) (2009) 827–845.

[121] N.H. Saeid, N. Hasan, M.H. Bin-Hj Mohd. Ali, Effect of the metallic foam heat sink shape on the mixed convection jet impingement cooling of a horizontal surface, J. Porous Media 21 (4) (2018) 295–309.
[122] J.M. Dixon, F.A. Kulacki, Mixed convection in fluid-superposed porous layers. Part 1. analysis, Int. J. Heat Mass Transfer 109 (2017) 1289–1300.
[123] J.M. Dixon, F.A. Kulacki, Mixed convection in fluid-superposed porous layers. Part 2. experiments, Int. J. Heat Mass Transfer 109 (2017) 1301–1306.
[124] B. Buonomo, V. Fardella, O. Manca, S. Nardini, S. Vigna, Investigation on thermal and fluid dynamic behaviours in mixed convection in horizontal channels with aluminium foam and heated from below, in: E3S Web of Conferences, Section of Heat Transfer and Fluid Dynamics, Vol. 197, Roma, 81031 Aversa (CE), Italy, 2020, p. 10006.
[125] S.A. Mohammed, G.F. Al-sumaily, H.A. Dhahad, M.C. Thompson, Heat transfer enhancement with pressure drop optimisation in a horizontal porous channel locally heated from below, Therm. Sci. Eng. Prog. 26 (2021) 101013.
[126] K. Vafai, Convective flow and heat transfer in variable porosity media, J. Fluid Mech. 147 (1984) 233–259.
[127] P. Cheng, C.T. Hsu, Fully-developed, forced convective flow through an annular packed-sphere bed with wall effects, Int. J. Heat Mass Transfer 29 (12) (1986) 1843–1853.
[128] C.H. Chen, T.S. Chen, C.K. Chen, Non-Darcy mixed convection along nonisothermal vertical surfaces in porous media, Int. J. Heat Mass Transfer 39 (6) (1996) 1157–1164.
[129] C.H. Chen, Mixed convection heat transfer from a horizontal plate with variable surface heat flux in a porous medium, Wärme- Und Stoffübertragung 34 (1) (1998) 1–7.
[130] F.C. Chou, P.Y. Chung, Effect of stagnant conductivity on non-Darcian mixed convection in horizontal square packed channels, Numer. Heat Transf.: A: Applications 27 (2) (1995) 195–209.
[131] P.Y. Chang, S.W. Shiah, M.N. Fu, Mixed convection in a horizontal square packed-sphere channel under axially uniform heating peripherally uniform wall temperature, Numer. Heat Transf.: A: Applications 45 (8) (2004) 791–809.
[132] N.H. Saeid, Analysis of mixed convection in a vertical porous layer using non-equilibrium model, Int. J. Heat Mass Transfer 47 (26) (2004) 5619–5627.
[133] N.J. Ahmed, I.A. Badruddin, J. Kanesan, K.S. Zainal, Study of mixed convection in an annular vertical cylinder filled with saturated porous medium, using thermal non-equilibrium model, Int. J. Heat Mass Transfer 54 (2011) 3822–3825.
[134] N.H. Saeid, Jet impingement interaction with cross flow in horizontal porous layer under thermal non-equilibrium conditions, Int. J. Heat Mass Transfer 50 (21-22) (2007) 4265–4274.
[135] K.C. Wong, N.H. Saeid, Numerical study of mixed convection on jet impingement cooling in a horizontal porous layer under local thermal non-equilibrium conditions, Int. J. Therm. Sci. 48 (5) (2009) 860–870.
[136] D.A.S. Rees, The effect of local thermal non-equilibrium on the stability of convection in a vertical porous channel, J. Porous Media 87 (2) (2011) 459–464.
[137] K.C. Wong, N.H. Saeid, Numerical study of mixed convection on jet impingement cooling in an open cavity filled with porous medium., Int. Commun. Heat Mass Transf. 36 (2) (2009) 155–160.
[138] B. Kotresha, N. Gnanasekaran, Determination of interfacial heat transfer coefficient for the flow assisted mixed convection through brass wire mesh, Int. J. Therm. Sci. 138 (2019) 98–108.
[139] M.K. Khandelwal, P. Bera, A thermal non-equilibrium perspective on mixed convection in a vertical channel, Int. J. Therm. Sci. 56 (2012) 23–34.
[140] B. Buonomo, O. Manca, P. Mesolella, S. Nardini, Local thermal non-equilibrium mixed convection in channels partially heated at uniform heat flux filed with a porous medium, in: Proceedings of ASME 12th Biennial Conference on Engineering Systems Design and Analysis, Vol. 3, Copenhagen, Denmark, 2014, ESDA2014–20538.
[141] B. Kotresha, N. Gnanasekaran, C. Balaji, Numerical simulations of flow-assisted mixed convection in a vertical channel filled with high porosity metal foams, Heat Transf. Eng. 41 (8) (2020) 739–750.
[142] V. Leela, K.N. Seetharamu, N. Kotloni, R.G. Reddy, Effect of asymmetrical wall heat flux and wall temperature ratio on mixed convection in a vertical micro-porous-channel with internal heat generation, Propuls. Power Res. 9 (4) (2020) 394–407.